

# Hyperpolarized $^{13}\text{C}$ MRI: Path to Clinical Translation in Oncology



John Kurhanewicz<sup>\*,1</sup>, Daniel B. Vigneron<sup>†,1</sup>,  
Jan Henrik Ardenkjaer-Larsen<sup>‡</sup>, James A. Bankson<sup>§</sup>,  
Kevin Brindle<sup>¶</sup>, Charles H. Cunningham<sup>#</sup>,  
Ferdia A. Gallagher<sup>\*\*</sup>, Kayvan R. Keshari<sup>††</sup>,  
Andreas Kjaer<sup>‡‡</sup>, Christoffer Laustsen<sup>§§</sup>,  
David A. Mankoff<sup>¶¶</sup>, Matthew E. Merritt<sup>##</sup>,  
Sarah J. Nelson<sup>†</sup>, John M. Pauly<sup>\*\*\*</sup>, Philips Lee<sup>†††</sup>,  
Sabrina Ronen<sup>†</sup>, Damian J. Tyler<sup>‡‡‡</sup>,  
Sunder S. Rajan<sup>§§§</sup>, Daniel M. Spielman<sup>¶¶¶</sup>,  
Lawrence Wald<sup>###</sup>, Xiaoliang Zhang<sup>†</sup>,  
Craig R. Malloy<sup>\*\*\*\*,1</sup> and Rahim Rizi<sup>¶¶,1</sup>

\*Department of Radiology and Biomedical Imaging, University of California San Francisco, San Francisco, CA, USA; †Department of Radiology and Biomedical Imaging, University of California at San Francisco, San Francisco, CA, USA; ‡Department of Electrical Engineering, Technical University of Denmark, Denmark; §Department of Imaging Physics, MD Anderson Medical Center, Houston, TX, USA; ¶Department of Biochemistry, University of Cambridge, Cambridge, UK; #Sunnybrook Health Sciences Centre, University of Toronto, Toronto, Canada; \*\*Department of Radiology, University of Cambridge, Cambridge, UK; ††Department of Radiology, Memorial Sloan Kettering Cancer Center, NY, New York, USA; †‡Department of Clinical Physiology, Nuclear Medicine & PET and Cluster for Molecular Imaging, Rigshospitalet and University of Copenhagen, Denmark; §§Department of Clinic Medicine, Aarhus University Hospital, Aarhus, Denmark; ¶¶Department of Radiology, University of Pennsylvania, PA, USA; ##Department of Biochemistry and Molecular Biology, University of Florida, Gainesville, FL, USA; \*\*\*Department of Electric Engineering, Stanford University, USA; †††Functional Metabolism Group, Singapore Biomedical Consortium, Agency for Science, Technology and Research, Singapore; ‡‡‡Department of Biomedical Science, University of Oxford, Oxford, UK; §§§Center for Devices and Radiological Health (CDRH), FDA, White Oak, MD, USA; ¶¶¶Departments of Radiology and Electric Engineering, Stanford University, USA; ###Department of Radiology, Harvard Medical School, Boston, MA, USA; \*\*\*\*Advanced Imaging Research Center, UT Southwestern Medical Center, Dallas, TX, USA

## Abstract

This white paper discusses prospects for advancing hyperpolarization technology to better understand cancer metabolism, identify current obstacles to HP (hyperpolarized)  $^{13}\text{C}$  magnetic resonance imaging's (MRI's)

widespread clinical use, and provide recommendations for overcoming them. Since the publication of the first NIH white paper on hyperpolarized  $^{13}\text{C}$  MRI in 2011, preclinical studies involving  $[1-^{13}\text{C}]$ pyruvate as well as a number of other  $^{13}\text{C}$  labeled metabolic substrates have demonstrated this technology's capacity to provide unique metabolic information. A dose-ranging study of HP  $[1-^{13}\text{C}]$ pyruvate in patients with prostate cancer established safety and feasibility of this technique. Additional studies are ongoing in prostate, brain, breast, liver, cervical, and ovarian cancer. Technology for generating and delivering hyperpolarized agents has evolved, and new MR data acquisition sequences and improved MRI hardware have been developed. It will be important to continue investigation and development of existing and new probes in animal models. Improved polarization technology, efficient radiofrequency coils, and reliable pulse sequences are all important objectives to enable exploration of the technology in healthy control subjects and patient populations. It will be critical to determine how HP  $^{13}\text{C}$  MRI might fill existing needs in current clinical research and practice, and complement existing metabolic imaging modalities. Financial sponsorship and integration of academia, industry, and government efforts will be important factors in translating the technology for clinical research in oncology. This white paper is intended to provide recommendations with this goal in mind.

*Neoplasia (2019) 21, 1–16*

## Introduction

Recent advances in cancer metabolism have generated considerable interest among clinicians.<sup>1,2</sup> However, the only imaging agent regularly used in the clinic to assess metabolism is the glucose analog  $[^{18}\text{F}]$  fluorodeoxyglucose (FDG), a positron emission tomography (PET) tracer that reports on local glucose uptake in many cancers, inflammation, and other processes. While FDG PET has been an extremely successful approach, it cannot assess downstream metabolism that is often important to more fully understand cancer. Hyperpolarized magnetic resonance imaging (HP MRI) provides a unique window into metabolic alterations based on its ability to measure molecular transformations of the imaging agent.<sup>3–6</sup> The method dramatically, although temporarily, increases MRI signal, which allows *in vivo* imaging of biologically active molecules that was impossible with conventional methods. Dynamic nuclear polarization of  $^{13}\text{C}$ -labeled biomolecules (probes) is currently the dominant hyperpolarization process used for preclinical work, and it is the only one that has been translated to patient studies. Due to space limitations, this white paper will focus on dynamic nuclear polarization–based polarization of  $^{13}\text{C}$  probes, although there are other methods to generate HP  $^{13}\text{C}$ -probes including *para*-hydrogen and brute force–based approaches,<sup>5,7–9</sup> and other nuclear magnetic resonance active nuclei such as  $^{129}\text{Xe}$ ,  $^{15}\text{N}$ , and  $^{31}\text{P}$  have been hyperpolarized.<sup>10,11</sup>

The potential to diagnose and better characterize cancer biology, predict cancer progression,<sup>12–17</sup> and monitor early response to treatment<sup>16,18–33</sup> using HP MRI was highlighted in the first NIH white paper on this technology in 2011. Since then, a polarizer capable of producing hyperpolarized material for human injection was commercially introduced, and the safety of hyperpolarized  $[1-^{13}\text{C}]$  pyruvate as a tool for measuring changes in tumor metabolism in patients was demonstrated.<sup>34</sup> This white paper will highlight preclinical advances, technical needs, and early experience with patients and discuss how HP MRI might fill existing needs in current clinical research and practice. Finally, we will examine obstacles to HP MRI's widespread clinical use and outline a path for clearing them.

## The Continuing Need for Animal Models

In addition to providing the only plausible method for testing the feasibility and safety of new HP molecular probes, preclinical animal studies are crucial for refining the methods for their use in specific diseases and for validating quantitative HP measurements of metabolism against tissue assays. Animal studies also provide the opportunity to better understand fundamental aspects of biochemistry and its modification by disease, therapy, nutritional state, and prescribed experimental conditions, which is possible in preclinical models but not in patients. Even if some HP probes prove inappropriate for clinical translation, their use in preclinical studies can still yield information of real clinical value by elucidating the metabolic pathways that novel treatment strategies could target.<sup>13,35,36</sup> Studies in animal models are also critical to drive basic science discovery of new metabolic drug interventions, where further applications of this technology might be beneficial in helping patients.

## HP Pyruvate for Diagnosis, Progression, and Response to Therapy

$[1-^{13}\text{C}]$ pyruvate was among the first HP probes introduced and remains the most widely studied in preclinical cancer models because it is easy to polarize,  $T_1$  is relatively long, and it occupies a critical branch point central to a number of significant metabolic pathways. Pyruvate is the product of glycolysis, and its major fates include reduction to  $[1-^{13}\text{C}]$ lactate via the enzyme lactate dehydrogenase (LDH) or oxidative metabolism to acetyl-coA with production of  $[^{13}\text{C}]$  bicarbonate in the mitochondria. Both processes result in an altered chemical shift that HP MRI is able to image at uniquely high temporal resolution. Although some exceptions have been observed,<sup>37,38</sup> the majority of preclinical cancer studies using HP pyruvate as a biomarker have shown increased conversion to HP lactate, consistent with the elevated lactate production (Warburg effect) that is an established characteristic of most cancerous cells.<sup>12–17,39–42</sup> These studies also demonstrated a mechanistic link between increased HP lactate signal and other cancer-associated cellular alterations such as the elevated expression of LDHA and monocarboxylate transporters, and lowered pH in the extracellular environment. The accompanying reduction in

pyruvate dehydrogenase activity can also be directly measured via appearance of HP [ $^{13}\text{C}$ ]bicarbonate from [ $1\text{-}^{13}\text{C}$ ]pyruvate or HP [ $5\text{-}^{13}\text{C}$ ]glutamate from [ $2\text{-}^{13}\text{C}$ ]pyruvate.<sup>19,20</sup>

Elevated transformation of hyperpolarized pyruvate to lactate has been established as a predictor of tumor progression in the transgenic adenocarcinoma of the mouse prostate "model" and genetically engineered pancreatic cancer models,<sup>43,44</sup> while a similar effect was also seen in longitudinal studies of liver cancer models,<sup>45</sup> alongside increased transamination of pyruvate to alanine. The latter effect appears to be specific to the hepatic tumor phenotype and may be diagnostic of tumor type or stage. These applications demonstrate HP MRI's value as a tool for prognosis and treatment planning. In addition, the ability to measure the metabolic information at a key branch point involved in downstream glucose metabolism provides information that is unique and complementary to FDG PET. HP [ $1\text{-}^{13}\text{C}$ ]pyruvate MRI provides insight into metabolism of a substrate other than glucose, and the synergistic combination of the two methods may offer significant advantages in identifying and characterizing cancer. For example, it was recently demonstrated in a PET/MRI study where FDG-PET and HP MRI were simultaneously acquired (hyperPET) that FDG-PET cannot demonstrate the Warburg effect per se but does discriminate between glycolysis and oxidative phosphorylation in contrast to HP MRI.<sup>46,47</sup>

HP MRI of pyruvate and its products is sensitive to the effects of anticancer therapies including DNA-damaging agents, radiotherapy, antivascular agents, targeted therapies, hormonal therapy, and antimetabolites—all of which have been reported to lead to a drop in HP lactate labeling, mediated by different mechanisms in the various treatments.<sup>9,11–25</sup> Additionally, the metabolism of HP fumarate to malate is sensitive to therapies that induce necrosis, such as VEGF neutralization and chemotherapy.<sup>31,33,48</sup> Despite some exceptions,<sup>38,48</sup> in general, preclinical data suggest that measurements from HP MRI of pyruvate predicts posttherapy cancer viability and aggressiveness. It will be important to preclinically test the hypothesis that therapeutic response can be determined at an earlier stage than that at which reduced tumor size is observable using anatomic imaging modalities as is done in the Response Evaluation Criteria in Solid Tumors approach.<sup>49</sup> Given the needs of a personalized approach to treatment, HP MRI's capacity to expedite assessment of response to therapy holds obvious value; this may be especially true in the case of early detection of nonresponse to therapy, which would enable more rapid adoption of alternate treatment strategies.

### Existing and Prospective Probes

Numerous molecules in addition to [ $1\text{-}^{13}\text{C}$ ]pyruvate have been successfully polarized and used to study multiple biological processes, including [ $2\text{-}^{13}\text{C}$ ]pyruvate, [ $1\text{-}^{13}\text{C}$ ]acetate, [ $1\text{-}^{13}\text{C}$ ]alanine, [ $^{13}\text{C}$ ]urea/[ $^{13}\text{C}$ ,  $^{15}\text{N}_2$ ]urea, perdeuterated [ $\text{U-}^{13}\text{C}_6$ ]glucose, [ $^{13}\text{C}$ ]bicarbonate, [ $1,4\text{-}^{13}\text{C}_2$ ]fumarate, and several others.<sup>50,51</sup> [ $1\text{-}^{13}\text{C}$ ]acetate has been used to study tricarboxylic acid cycle flux and fatty acid oxidation in heart and skeletal muscles through its conversion to acetyl-CoA by acetyl-CoA synthase,<sup>52,53</sup> while HP butyrate has been utilized to study ketone body metabolism and short-chain fatty acid pathways.<sup>54</sup> HP alanine has been employed as an alternate probe to study metabolism in the muscle and liver.<sup>55,56</sup> HP glucose has been used to monitor flux via the pentose phosphate pathway, as well as glycolytic flux and lactate production<sup>57,58</sup>; [ $1\text{-}^{13}\text{C}$ ]dehydroascorbate has been imaged and used to monitor intercellular redox status

and to inform on response to treatment by measuring the modulation of the tumor microenvironment<sup>59–61</sup>; HP [ $1\text{-}^{13}\text{C}$ ]alpha-ketoglutarate has been used to track the neomorphic oncogenic activity of mutant IDH via its metabolism to the oncometabolite 2-hydroxyglutarate and glutamate.<sup>62,63</sup> More recently, HP [ $1\text{-}^{13}\text{C}$ ]glutamine has been used to directly measure metabolic flux to 2-hydroxyglutarate, demonstrating a methodology to trace nutrient of origin to a product *in vivo*.<sup>64</sup> HP [ $2\text{-}^{13}\text{C}$ ]dihydroxyacetone has been used to assess hepatic gluconeogenesis,<sup>65</sup> while HP acetoacetate has been proposed as an indicator of mitochondrial redox status, although its utility has not yet been studied in tumors.<sup>66</sup> The utility of inert metabolic probes such as  $^{13}\text{C}$ -urea or  $^{13}\text{C}$ ,  $^{15}\text{N}_2$ -urea has also been shown in simultaneous acquisitions with metabolized species as a means to normalize delivered agent concentration and uptake kinetics, or as independent markers of perfusion in tumor tissue.<sup>67</sup> This combined acquisition has the potential to alleviate technical challenges in accurately determining metabolic and hemodynamic changes associated with treatment response.<sup>68–70</sup>

Numerous biologically relevant, potentially polarizable molecules remain unstudied,<sup>71</sup> and new HP probes to detect and assess response to various types of cancer treatment are urgently needed. For example, because MRI of HP pyruvate is unable to differentiate increased lactate production associated with tumor cells from that associated with inflammatory cells, other probes—such as the recently tested HP [ $6\text{-}^{13}\text{C}$ ]arginine—are necessary for monitoring response to therapies that target this cell type.<sup>72</sup> In addition, the development of hyperpolarized biomarkers capable of monitoring response to the most promising immunotherapies currently in use, such as checkpoint inhibitors, is a major unmet need which should command immediate preclinical attention. Probes tailored to the innate or designed metabolic characteristics of such cellular therapeutic agents would be extremely valuable for assessing treatment efficacy at a very early stage.

### Further Avenues of Preclinical Animal Study

Preclinical animal studies enable investigation of appropriate methods to report HP data or integrate multiple HP measurements, for example, through the development and testing of methods for the true simultaneous measurement of perfusion and metabolism to improve quantitation<sup>69</sup> and facilitate identification of poorly perfused but metabolically active disease that is often highly aggressive and difficult to treat.<sup>73</sup> The possibility of acquiring such a combined measurement was demonstrated using copolarized [ $1\text{-}^{13}\text{C}$ ]pyruvate and  $^{13}\text{C}$  urea in rats: metabolic alterations were registered via the conversion of pyruvate into  $^{13}\text{C}$  bicarbonate, while alterations in perfusion were measured via changes in myocardial signals of pyruvate and urea.<sup>60</sup> The development of HP probes and pulse sequences capable of simultaneously measuring perfusion/metabolism mismatch in cancerous tissue has the potential to provide valuable information regarding tumor heterogeneity, with obvious implications for the development of more sensitive and personal treatment.<sup>73</sup> Similar possibilities exist for additional ratiometric measurements (e.g., local pH derived from  $\text{CO}_2\text{:HCO}_3$  ratio,<sup>74–78</sup> or redox state in different intracellular compartments derived from lactate:pyruvate ratio,<sup>37,79,80</sup>  $\alpha$ -ketoisocaproate:leucine ratio,<sup>81,82</sup> or ascorbate:dehydroascorbate ratio).<sup>59,60</sup> These combinations are being explored or developed in animal, organ, and cell research models with the potential for future clinical application. The unique ability to image multiple metabolites simultaneously—either through the injection of a single hyperpolarized agent that is variously metabolized or via the injection of several HP agents at once—means that HP MRI technology

is particularly suited to this kind of combined measurement. Because radiometric measurements are potentially subject to bias in the case of differing uptake or relaxation characteristics, preclinical models are critical for validation using histological and invasive techniques that are not practical in human subjects.

In addition to exploring HP technology, preclinical animal studies enable measurements that are not feasible in human subjects for reasons such as invasiveness, toxicity, or the current inability to hyperpolarize substrates in sufficient volume. Studies using genetically engineered and patient-derived xenograft models enable the combined use of PET and HP MRI, as well as the collection of a robust spectrum of supporting *in vivo* and histological measurements, including metabolite and enzyme profiles as well as histochemical measurements of enzyme heterogeneity, which can both confirm and enhance the data collected via these primary imaging modalities. While the ability to collect such supplementary measurements is undoubtedly crucial to validating the accuracy of primary measurements enabled by HP probes, its ultimate value may lie in the more general expansion of our understanding of the biochemical properties characteristic of specific disorders. For example, HP probes are currently being used to assess the progression of lung<sup>83</sup> and brain<sup>84</sup> injury, yielding valuable insights into the mechanism of injury propagation. While these studies are not directly applicable to imaging human injury using HP agents in the clinic, the information gained will help guide therapeutic approaches that could have significant clinical impact.

### Needs and Future Directions

There is substantial need for preclinical polarizers capable of achieving high polarization and tailored for producing masses of material suitable for rodent exams. Such a polarizer that is less expensive than a clinical device would dramatically expand preclinical efforts and speed clinical investigations. High levels of polarization increase the signal-to-noise ratio and potentially open up previously undetectable biological pathways for study. High levels of polarization may also allow a reduction in the injected probe concentration. HP probes are injected at physiologic or supraphysiologic doses, and preclinical studies investigating the extent to which physiologic concentrations of HP probe might perturb *in vivo* metabolism relative to a tracer approach like PET are key to the proper interpretation of HP MRI findings. As previous work has demonstrated, this increased polarization is most easily achieved by employing higher magnetic fields and lower temperatures during the polarization process.<sup>85,86</sup>

Optimized pulse sequences can also be used to preserve the magnetization of specific hyperpolarized substrates while enhancing the detection of products.<sup>4,87</sup> Since the lack of standardized techniques remains an obstacle to the growth of HP MRI as a field of study, this represents a potential opportunity for the research community to collaborate with small imaging system manufacturers on the creation of standard imaging sequences and basic processing protocols, thereby possibly expanding the use of HP MRI techniques beyond labs with a strong MRI physics focus. Other beneficial technical improvements would include the development of a less complex user interface, as well as a more direct, rapid mechanism for the delivery of polarized agents into the animal or cell or tissue culture bioreactor.

The development and optimization of new hyperpolarized molecular probes, and preclinical studies that accurately recapitulate

important aspects of human disorders—whether using primary cells and tissues, genetically engineered, patient-derived xenograft, or other models—continue to be of great value. Robust mechanistic validation linking hyperpolarized metabolic observations to established biological events are also essential to establish the value of hyperpolarized imaging approaches and their potential limitations. Significant effort is currently under way—and should be further encouraged—to explore the use of HP imaging biomarkers to inform on a variety of disease conditions and therapeutic strategies and to integrate this unique new information to positively affect outcome. The combined use of targeted therapeutic approaches and HP MRI in these models will provide a framework for accessing HP biomarkers of treatment response for clinical translation. It is also important to conduct more studies to validate the use of HP MRI in combination with other imaging modalities such as PET, as was recently done during a single imaging session in a canine cancer model.<sup>46,47</sup> The value of combining these measurements lies not only in a more complete characterization of the cancerous tissue being imaged but in reduced scan time and more efficient use of resources.

### Necessary Technical and Analytic Developments

Success with preclinical studies encouraged a more translational focus. In order to enable clinical trials, several specific technical developments were necessary. In the following section, we will outline some of the recent technical progress and note additional opportunities.

#### A Device for Polarization

Over the past 10 years, there have been significant improvements in polarizer hardware, from initial prototypes suitable for rodent exams to current commercial products that can support human studies.<sup>88</sup> The performance in terms of polarization and speed of delivery has been adequate for initial [1-<sup>13</sup>C]pyruvate studies, but further developments are needed to achieve higher and faster polarizations reliably with increased cost-effectiveness, and to streamline methods of HP probe sterile delivery for pyruvate and other HP probes for future clinical research. Next-generation polarizers that are optimized for preclinical research will also be vital for supporting the development of new hyperpolarized agents and their use in basic science and translational research.

#### Imaging Hardware

Another important commercial goal should be improved <sup>13</sup>C MR imaging hardware. While each major MR scanner vendor offers product hardware enabling the excitation and detection of hyperpolarized signals at the <sup>13</sup>C frequency, several additional modifications would significantly improve the performance and applicability of this technology. Commercially available double-tuned body coils would greatly benefit human studies by allowing uniform excitation for <sup>13</sup>C over any target disease site, as is the case for conventional <sup>1</sup>H MRI. Current studies have been limited by both the <sup>13</sup>C detector hardware and short acquisition times due to metabolism, signal relaxation, and excitation losses; thereby necessitating the use of strategies that more efficiently encode magnetization.<sup>69,89,90</sup> As in <sup>1</sup>H MRI, detector arrays with a high number of elements can facilitate higher acceleration rates to generate images faster and with increased spatial coverage and resolution. For optimal clinical studies, scanners with a greater number of receive channels (at least 32 channels) are needed to support <sup>13</sup>C detector arrays with geometries that are optimized for all

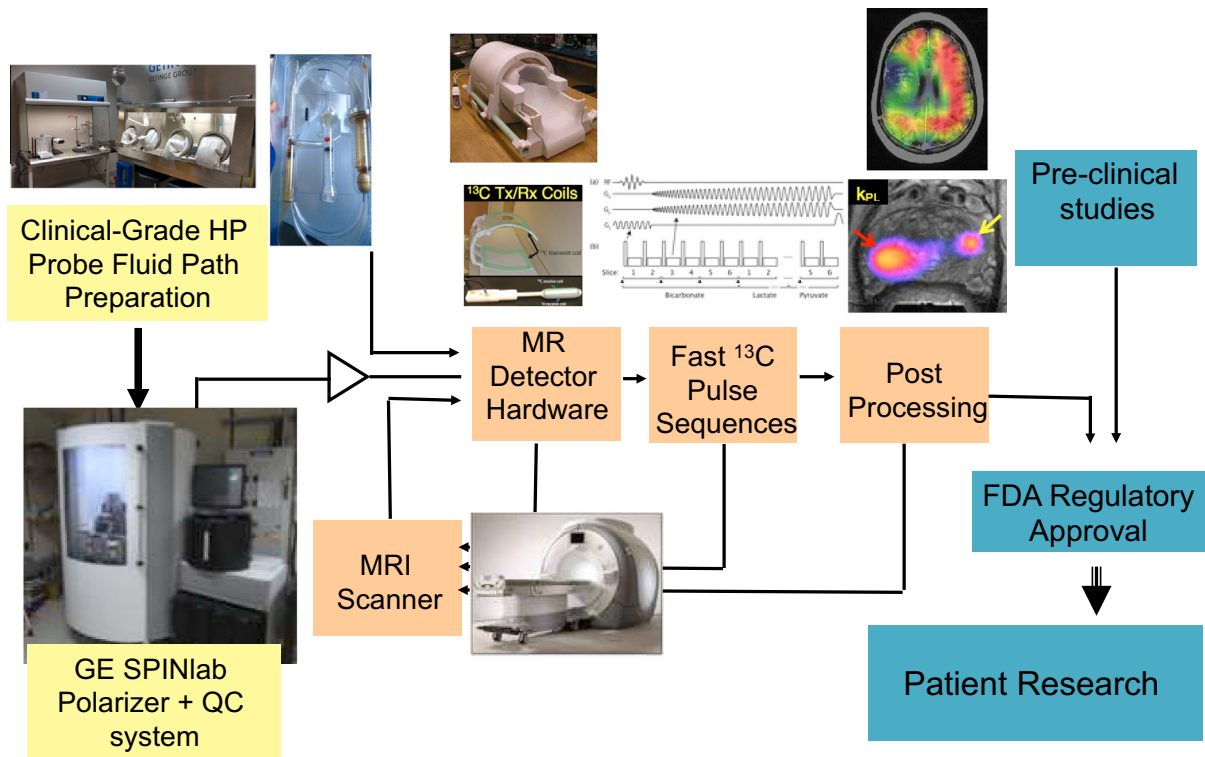


**Figure 1.** Schematic showing the required components for HP  $^{13}\text{C}$  MRI clinical translation. Thirty-two-channel head coil.

body regions. Dual-tuned or nested receive arrays that would permit high-quality “standard of care”  $^1\text{H}$  MRI alongside sensitive  $^{13}\text{C}$  detection without repositioning or replacing coils in order to enhance patient comfort and workflow. Higher-performance gradients will also be critical for improving the speed, coverage, and performance of HP  $^{13}\text{C}$  MRI, which requires four times higher gradient strengths to achieve the same effect as for  $^1\text{H}$  MRI. The progress seen in highly parallel acquisition of  $^1\text{H}$  MRI over the past few years provides reason to believe that these radiofrequency (RF) coil challenges can be met within the constraints imposed by currently available gradient bores. The increased costs would be a very small fraction of total system cost and easily justified by the greatly enhanced capabilities. The development of appropriate phantoms that enable testing of new techniques for HP  $^{13}\text{C}$  MRI prior to human studies is also important for advancing the field. Static phantoms containing  $^{13}\text{C}$ -enriched compounds facilitate technical development and quality assurance testing to confirm scanner and coil performance at thermal equilibrium, while dynamic phantoms that simulate the kinetics of chemical conversion *in vivo*<sup>91</sup> are important to develop and validate quantitative dynamic imaging measurements.

#### Acquisition Methods for Human Studies

The high signal-to-noise ratio provided by this hyperpolarization technique makes high-resolution acquisitions feasible. However, rapid metabolism and short  $T_1$  relaxation times can limit the matrix size—and thus the spatial resolution and coverage possible—with conventional phase-encoding. The MR acquisition techniques used for initial animal studies and the first human trial<sup>34</sup> were limited in spatial coverage (typically <8 cm) and dynamic temporal information. This clinical trial used single-slice dynamic  $^{13}\text{C}$  echo-planar

spectroscopic imaging (EPSI) in some patients to estimate the correct starting time for a 12-second 3D EPSI single time-point acquisition in subsequent patients with a small FOV of 8-10 cm.<sup>34</sup> Dynamic 1D EPSI measurements efficiently encode frequency and space along the readout direction following a single excitation. Extension to multiple spatial dimensions requires additional excitations and phase encoding repetitions for each dynamic time point. New acquisition and analysis techniques are needed for volumetric, dynamic HP MR data with improved spatial coverage and temporal resolution. Most preclinical and clinical research studies have used spectroscopic-based acquisitions, but imaging-based acquisitions including balanced steady-state free precession sequences,<sup>92,93</sup> spectral-selective echo-planar,<sup>94</sup> and spiral trajectories<sup>68,95-97</sup> have clear advantages in terms of speed and ease of implementation and analysis. Methods combining  $^{13}\text{C}$  and  $^1\text{H}$  excitation and reception could benefit the detection of many metabolites via decoupling and indirect detection.<sup>98,99</sup>

#### Reconstruction, Dynamic Modeling, and Enzyme Rate Constants

Ideal dynamic MRSI data would be resolved in three spatial dimensions, the spectral dimension, and time with adequate coverage and speed to enable reliable quantification of metabolic parameters. Fortunately, the spectrum is sparse, with only a few spectral lines. In addition, the time dimension is slowly varying. These two features allow the amount of encoding required to be greatly reduced by using compressed sensing reconstructions along with low-rank or model-based reconstruction in the temporal dimension.<sup>89,100,101</sup> Spatial data reduction strategies, including parallel and constrained imaging methods, are crucial for reducing the number of excitations that are necessary to reconstruct dynamically changing data.<sup>102</sup> Fewer

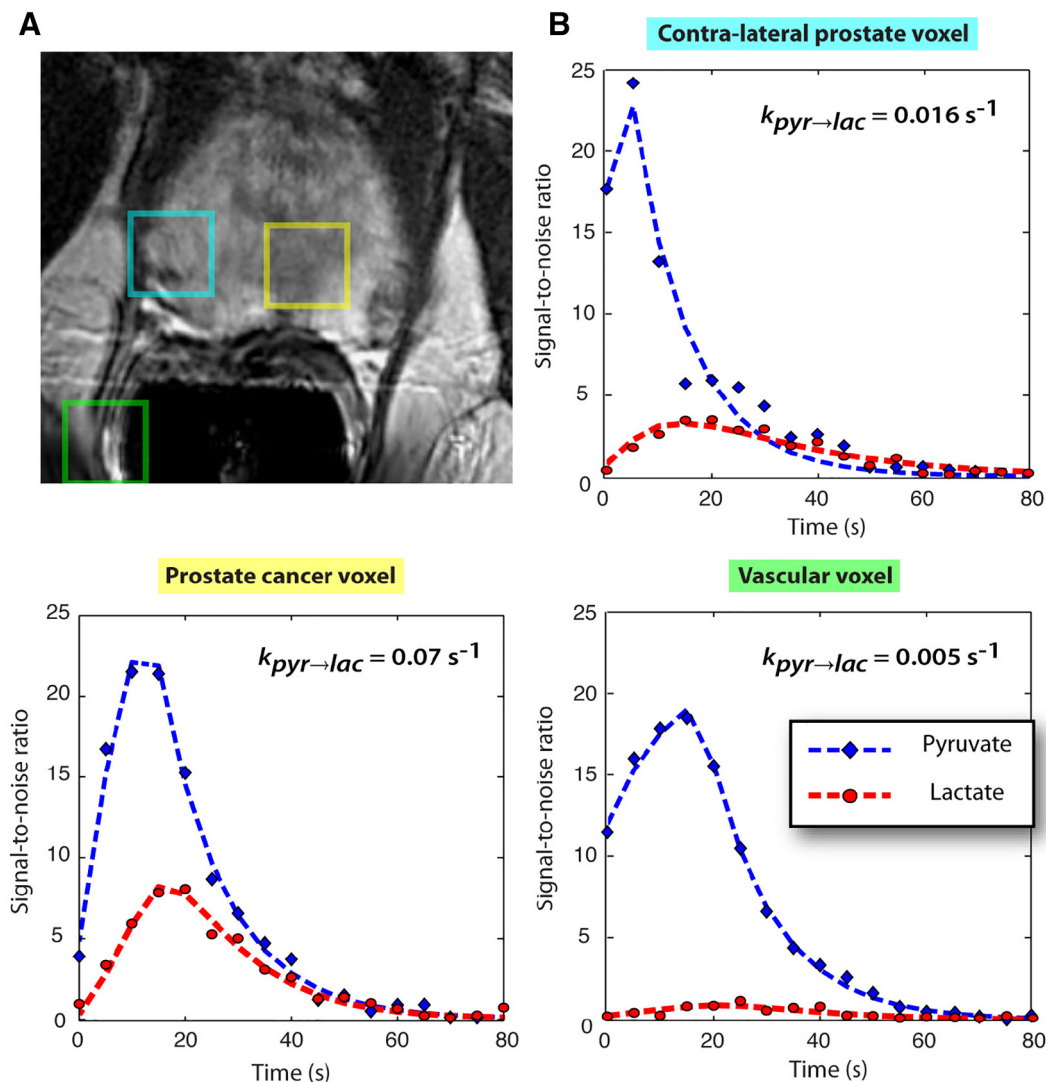


**Figure 2.** Images are from a representative patient with a current PSA of 3.6 ng/ml, who had biopsy-proven prostate cancer in the left apex (Gleason grade 3 + 4) and received the highest dose of hyperpolarized [1-<sup>13</sup>C]pyruvate (0.43 ml/kg). (A) A focus of mild hypointensity can be seen on the T<sub>2</sub>-weighted image, which was consistent with the biopsy findings. (B to D) 2D localized dynamic hyperpolarized [1-<sup>13</sup>C] pyruvate and [1-<sup>13</sup>C]lactate from spectral data that were acquired every 5 seconds from voxels overlapping the contralateral region of prostate (turquoise), a region of prostate cancer (yellow), and a vessel outside the prostate (green). The dynamic data were fit to provide  $k_{PL}$  as described previously.<sup>139</sup> Figure taken from Nelson SJ, Kurhanewicz J, Vigneron DB, Larson PEZ, Harzstark AL, Ferrone M, et al. Metabolic Imaging of Patients with Prostate Cancer Using Hyperpolarized [1-<sup>13</sup>C]Pyruvate. *Science Translational Medicine* 2013;**5**:198ra108-198ra108.

excitation pulses preserve HP magnetization, allowing for increased coverage, higher excitation angles, or prolonged interaction with target biology. Optimized excitation schemes are required to permit further sensitivity enhancement.

Parallel imaging reconstructions can be challenging since signal at thermal equilibrium is too weak for practical measurement of sensitivity maps. Autocalibrating methods such as GRAPPA (GeneRalized Autocalibrating Partial Parallel Acquisition) can avoid wasting polarization and imaging time acquiring sensitivity maps but can be problematic because the fully sampled central region can be a large fraction of the sampled k-space volume which limits acceleration. Care must also be taken to ensure that undersampled parallel imaging data are acquired in such a way that the data are self-consistent enough to satisfy fundamental assumptions about the relationship between undersampled data. Alternatively, undersampled k-space data can be used

to compute the coil sensitivities as with a calibration-less approach for HP <sup>13</sup>C MR.<sup>103</sup> Further investigations are needed to develop acquisition strategies that minimize uncertainty while maximizing the efficiency of spatial, temporal, and spectral encoding—including methods that exploit redundant information that could be derived from conventional <sup>1</sup>H MRI.

MRI of hyperpolarized substrates is unique among diagnostic imaging modalities in its ability to provide information about dynamic chemical interactions and imaging agent metabolism. New approaches for characterizing the transient interaction between the imaging agent and targeted biological processes are therefore required. A variety of approaches have been proposed, including semiquantitative area under the curve measurements—such as the normalized lactate ratio—that reflect the ratio of locally observed product to precursor and product, “snapshot” measurements of metabolite

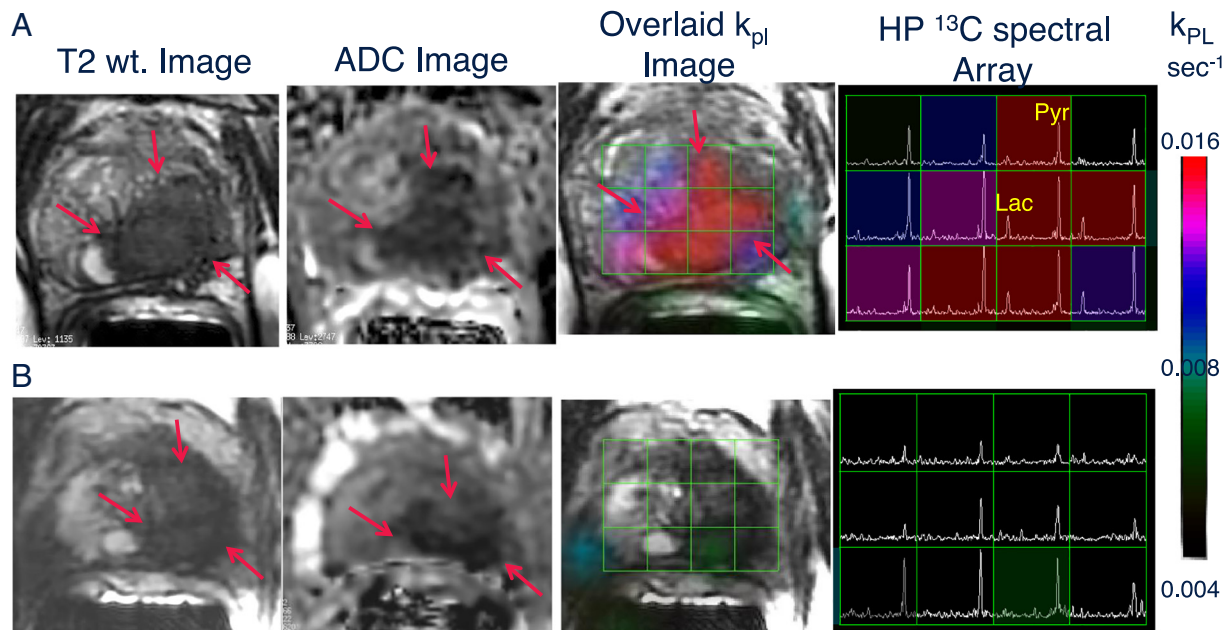


**Figure 3.** Representative axial  $T_2$ -weighted anatomic image and corresponding water apparent diffusion coefficient (ADC) image and  $T_2$ W image with an overlaid pyruvate-to-lactate metabolic flux ( $k_{PL}$ ) image and corresponding HP  $^{13}C$  spectral array for a 52-year-old prostate cancer patient with extensive high-grade prostate cancer (A) before therapy and (B) 6 weeks after initiation of androgen ablation and chemotherapy. Before treatment, the region of prostate cancer can be clearly seen (red arrows) as a reduction in signal on the  $T_2$ W and ADC images, and increased HP lactate and associated  $k_{PL}$  on. Pretreatment, HP  $[1-^{13}C]$ pyruvate CS-EPSI demonstrated a large region of high HP Lac/Pyr ratio, resulting in a high  $k_{PL}$ , which is consistent with region of decreased  $T_2$  MRI signal and water ADC associated with biopsy-proven Gleason 4 + 5 prostate cancer. At 6 weeks after initiation of androgen deprivation therapy, repeat HP  $^{13}C$  MRI demonstrated nearly complete abrogation of elevated HP lactate peaks and associated near-complete diminution of intratumoral  $k_{PL}$  values on dynamic imaging ( $k_{PL}$  max  $0.025\text{ s}^{-1}$  at baseline and  $0.007\text{ s}^{-1}$  on follow-up). Notably, there were negligible change in size of tumor on  $T_2$ -weighted MRI and only a modest change on ADC imaging, supporting the ability of HP  $^{13}C$  MRI to detect early metabolic responses before such a response can be ascertained using standard radiographic criteria. Concordant with these findings, the patient subsequently achieved a marked clinical response, with an undetectable serum PSA nadir at 6 months after ADT initiation. Figure taken from Aggarwal, R., Vigneron, D.B., and Kurhanewicz, J. Hyperpolarized  $[1-^{13}C]$  Pyruvate Magnetic Resonance Imaging Detects an Early Metabolic Response to Androgen Ablation Therapy in Prostate Cancer, *Eur Uro*, July 23, 2017;72(6)1028-1029. PMID:5723206.

distribution, or ratiometric values at a single time point.<sup>34</sup> Pharmacokinetic analysis of dynamic multispectral data has shown the ability in both preclinical and human studies (Figure 1) to derive rate constants for substrate conversions such as  $k_{PL}$ , the spectroscopic/imaging biomarker for the calculated rate at which HP pyruvate is converted into lactate.<sup>18,34,69,104,105</sup> Quantitative measures such as  $k_{PL}$  can provide important quantitative parameters for many applications where precise measurements are needed to quantify changes in specific drivers of aerobic glycolysis. Recent literature shows the strong correlation between perfusion and metabolic measures of  $k_{PL}$ <sup>69,94</sup> with cancer aggressiveness and response to therapy. To realize the inherent promise of the unprecedented new information afforded by HP substrates, further research is critically needed to develop and test new accurate, reproducible quantitative analysis methods.

Once achieved, the technical and analytical developments outlined above should help to significantly accelerate the translation of HP  $^{13}C$  MRI to the clinic and increase its biomedical value—both by enabling studies which offer further proof of the improved molecular imaging capabilities it has already displayed and by optimizing their potential clinical utility.

### Translation to Patients with Cancer

The first-in-human study convincingly demonstrated that injection of HP  $[1-^{13}C]$ pyruvate is safe and that imaging metabolic products of

hyperpolarized  $[1-^{13}C]$ pyruvate metabolism is feasible<sup>34</sup>. Since then, a number of significant technical improvements relevant to improving data quality and preserving safety have been implemented. These include improved technology and strategies for generating sterile hyperpolarized material using a commercial device, the SPINlab, new MR data acquisition sequences, and multichannel  $^1H/^{13}C$  radio frequency RF coils. Pictured in Figure 2 is the workflow for the current-generation SPINlab which is now used routinely in patient studies and provides automated polarization, dissolution, and quality assurance system. The SPINlab polarizer uses a 5-T magnetic field and operates at  $\sim 0.8\text{ K}$ . It has the capacity to polarize up to four samples simultaneously, thus opening the door for the injection of multiple HP probes within a single imaging exam. A critical part of the SPINlab polarization and quality assurance process is the fluid path that enables polarization in a closed system to minimize the potential for microbial contamination. Compared to the initial human study using a prototype polarizer in a clean room, the achievable polarization of  $[1-^{13}C]$ pyruvate has more than doubled (from  $\sim 18\%$  to  $\sim 40\%$ ), and the time to delivery of HP  $^{13}C$  pyruvate was reduced (from  $\sim 68$  seconds to  $\sim 55$  seconds). Around the world, seven sites have performed human exams using the SPINlab polarizer, and more than 20 have been installed.

While initial patient studies have focused on  $[1-^{13}C]$ pyruvate,  $[2-^{13}C]$ pyruvate has recently been FDA approved and is being added

**Table 1.** Current Hyperpolarized <sup>13</sup>C MRI Clinical Trials—*ClinicalTrials.gov*

Hyperpolarised 13C-Pyruvate MRI Study	Cancer Cardiovascular diseases	University College London, London, UK
Effect of Cardiotoxic Anticancer Chemotherapy on the Metabolism of [1- <sup>13</sup> C]Pyruvate in Cardiac Mitochondria	Breast neoplasms	UT Southwestern—Advanced Imaging Research Center, Dallas, TX, USA
Hyperpolarized Carbon C 13 Pyruvate Magnetic Resonance Spectroscopic Imaging in Predicting Treatment Response in Participants With Prostate Cancer	Prostate adenocarcinoma PSA level greater than 10 Stage IIB prostate cancer AJCC v8 (and 7 more...)	M D Anderson Cancer Center, Houston, TX, USA
Hyperpolarized Carbon C 13 Pyruvate Magnetic Resonance Spectroscopic Imaging in Detecting Lactate and Bicarbonate in Participants With Central Nervous System Tumors	Malignant central nervous system neoplasm Metastatic malignant neoplasm in the central nervous system	Stanford University School of Medicine Palo Alto, CA, USA
Imaging of Traumatic Brain Injury Metabolism Using Hyperpolarized Carbon-13 Pyruvate	Traumatic brain injury	UT Southwestern—Advanced Imaging Research Center Dallas, TX, USA
Effect of Fatty Liver on TCA Cycle Flux and the Pentose Phosphate Pathway	Fatty liver	
Role of Hyperpolarized 13C-Pyruvate MR Spectroscopy in Patients With Intracranial Metastasis Treated With (SRS)	Brain metastases	Sunnybrook Health Sciences Centre Toronto, Ontario, Canada
Hyperpolarized 13C MR Imaging of Lactate in Patients With Locally Advanced Cervical Cancer (LACC) Cervical Cancer	Uterine cervical neoplasms	Sunnybrook Health Sciences Centre Toronto, Ontario, Canada
Study to Evaluate the Feasibility of 13-C Pyruvate Imaging in Breast Cancer Patients Receiving Neoadjuvant Chemotherapy	Breast cancer	Sunnybrook Health Sciences Centre Toronto, Ontario, Canada
Metabolic Characteristics of Brain Tumors Using Hyperpolarized Carbon-13 Magnetic Resonance Spectroscopic Imaging (MRSI)	Brain tumor adult	
UTSW HP [13-C] Pyruvate Injection in HCM	Cardiomyopathy, hypertrophic	UT Southwestern Medical Center - Advanced Imaging Research Center Dallas, TX, USA
Pilot Study of Safety and Toxicity of Acquiring Hyperpolarized Carbon-13 Imaging in Children With Brain Tumors	Pediatric brain tumors	UCSF Helen Diller Family Comprehensive Cancer Center, San Francisco, CA, USA
Hyperpolarized C-13 Pyruvate as a Biomarker in Patients With Advanced Solid Tumor Malignancies	Prostate cancer	University of California, San Francisco San Francisco, CA, USA
Magnetic Resonance (MR) Imaging With Hyperpolarized Pyruvate (HP) ( <sup>13</sup> C) in Castration-Resistant Prostate Cancer	Prostate cancer	University of California, San Francisco San Francisco, CA, USA
Hyperpolarized Carbon-13 Imaging of Metastatic Prostate Cancer	Prostate cancer	Sunnybrook Health Sciences Centre Toronto, Ontario, Canada
Metabolic Imaging of the Heart Using Hyperpolarized ( <sup>13</sup> C) Pyruvate Injection	Hypertension Hypertrophy	Sunnybrook Health Sciences Centre Toronto, Ontario, Canada
Multiparametric MRI for Prostate Cancer Localization and Characterization Using Hyperpolarized Pyruvate ( <sup>13</sup> C) Injection	Prostatic neoplasms	Sunnybrook Health Sciences Centre Toronto, Ontario, Canada
A Pilot Study of (MR) Imaging With Pyruvate ( <sup>13</sup> C) to Detect High Grade Prostate Cancer	Prostate cancer	University of California, San Francisco San Francisco, CA, USA
MRI With C13 Pilot Study Prostate Cancer	Prostate cancer	University of California, San Francisco San Francisco, CA, USA
Characterization of Hyperpolarized Pyruvate MRI Reproducibility	Malignant solid tumors	Memorial Sloan Kettering Cancer Center New York, NY, USA
Hyperpolarized Pyruvate Injection in Subjects With Prostate Cancer	Prostate cancer	University of California San Francisco

to [1-<sup>13</sup>C]pyruvate in ongoing clinical trials. Additionally, funded clinical research studies are working toward the use of <sup>13</sup>C urea, [5-<sup>13</sup>C]glutamine, [1-<sup>13</sup>C]alpha-ketoglutarate, and [1,4-<sup>13</sup>C<sub>2</sub>]fumarate in patient studies. To aid with submitting investigator-initiated Investigational New Drug (IND) applications for future patient studies, the IND for the use of [1-<sup>13</sup>C]pyruvate was transferred to the NCI and is available on the following website ([https://imaging.cancer.gov/programs\\_resources/cancer-tracer-synthesis-resources/hyperpolarized-C13-pyruvate-documentation.htm](https://imaging.cancer.gov/programs_resources/cancer-tracer-synthesis-resources/hyperpolarized-C13-pyruvate-documentation.htm)).

### Early Patient Validation Studies

Early patient validation studies involving test-retest reproducibility, correlations with pathologic findings, and clinical outcomes such as survival and disease progression after treatment have been initiated (data available from [clinicaltrials.gov](https://clinicaltrials.gov)). In a study utilizing 2D dynamic EPSI of preprostatectomy prostate cancer patients (NCT02421380), time to max pyruvate was reproducible when corrected for the arterial input function with no significant difference observed in repeat injections of the same patient within the same exam.<sup>106</sup> In two recent clinical trials of prostate cancer patients preprostatectomy (NCT02526360) and before and after treatment (NCT02911467), a 3D dynamic compressed sensing EPSI sequence

was used to obtain full prostate coverage and to model the apparent rate of pyruvate to lactate conversion,  $k_{PL}$ . In the setting of advanced prostate cancer, early (6 weeks) after effective androgen deprivation therapy, there was a significant early reduction in  $k_{PL}$  that receded changes in mp-<sup>1</sup>H MRI and predicted clinical response (Figure 3).<sup>107</sup> Comparison with current state-of-the-art imaging modalities such as <sup>1</sup>H MRI is key to determining the added value of HP <sup>13</sup>C MRI, and with current HP <sup>13</sup>C MRI studies expanding to metastatic sites within the body,<sup>108,109</sup> the synergy of HP MRI with currently used PET probes will also need to be investigated.

There are currently a number of single-institution HP <sup>13</sup>C MRI clinical trials in the setting of breast, cervical, liver, and brain cancer, and an initial multisite clinical trial for prostate cancer (Table 1). Following promising preclinical studies in brain tumors, multiple sclerosis, and traumatic brain injury, the feasibility of using HP <sup>13</sup>C MRI for evaluating brain metabolism in patient studies was recently demonstrated.<sup>110,111</sup> These studies demonstrated that [1-<sup>13</sup>C] pyruvate are transported across the blood brain barrier and that conversion to [1-<sup>13</sup>C]lactate can be detected in regions of both tumor and normal brain. Interestingly, the rate of conversion in normal brain was substantially higher than had previously been observed in anesthetized preclinical models. For dynamic slab-localized and 2-D



echo planar spectroscopic imaging data with 4–8 ml spatial resolution, it was also possible to observe the conversion of HP pyruvate to bicarbonate, which may discriminate between tumor and normal brain. Additional studies are needed to optimize the pulse sequences, RF coils, and experimental design to observe all three resonances at a finer resolution and with volumetric coverage. Single-institution studies that have been funded by the NIH include protocols for obtaining data from the normal brain, in primary brain tumors prior to image-guided surgery, and for comparing that conversion to [1-<sup>13</sup>C]lactate/[1-<sup>13</sup>C]pyruvate in patients pre- and posttreatment with radiation and temozolomide.

There are also several clinical trials investigating noncancerous diseases, such as cardiomyopathy, hypertrophy and hypertension, and fatty liver disease (Table 1). Altered cardiac energetics is known to play an important role in the progression toward heart failure, and a recent study demonstrated the feasibility of assessing pyruvate metabolism *in vivo* in humans.<sup>97</sup> The appearance of <sup>13</sup>C-bicarbonate signal after administration of hyperpolarized [1-<sup>13</sup>C]pyruvate was readily detected in a cohort of healthy controls, suggesting that this technology may 1 day allow a direct measure of flux through the PDC in the *in vivo* human myocardium, providing a means for understanding therapeutic approaches that target metabolism.

While prior and ongoing HP <sup>13</sup>C MRI patient studies have addressed many of the initial obstacles, there remain a number of challenges to the robust clinical translation of hyperpolarized [1-<sup>13</sup>C] pyruvate MRI and its full FDA approval, as well as the translation of other new hyperpolarized probes into the clinic. These challenges are discussed in the following section.

### Challenges in Translation to Clinical Research and Practice

Compared to current metabolic imaging methods based on positron tomography, HP <sup>13</sup>C MRI technology offers superior information yield about fluxes in metabolic pathways without the constraints of ionizing radiation. Nevertheless, while other potential benefits such as safety and patient acceptability may be substantial, the central question for clinical translation is whether HP <sup>13</sup>C MRI provides actionable clinical information that is inaccessible by other methods. In examining how this question can be answered in the affirmative, we can take some cues from the use of FDG PET/CT.<sup>112,113</sup>

#### The Clinical Role of Imaging in Cancer

The traditional clinical roles for imaging in cancer are detection, diagnosis, staging, and monitoring therapy.<sup>114</sup> More specifically, imaging techniques are typically used in the clinic to detect the tumor through screening; to guide cancer diagnosis, including tissue sampling; and to determine the extent of cancer spread. More recently, molecular imaging in particular has been used as a cancer biomarker to help direct treatment.<sup>115,116</sup> Already demonstrated in animal models<sup>20</sup> and initial patient studies,<sup>107</sup> this capacity to rapidly detect response to treatment is perhaps the most promising in terms of clinical translation. Because a response to therapy prior to any change in tumor volume could occur within days, or even hours, the ability to detect this change could redirect therapy to improve therapeutic efficacy and avoid unnecessary toxicity for ineffective treatments, potentially saving lives and alleviating suffering.

The complexity, expense, and requirement for administering an imaging agent will likely limit HP MRI's role as a primary screening tool. However, coupled to blood or urine metabolic biomarkers

indicative of cancer risk and specific cancer metabolic signatures,<sup>117</sup> HP MRI could provide a very powerful, targeted detection tool in stratified populations. It could play a key role in diagnosis, for example, as metabolic features identified by HP MRI might provide a both sensitive and specific means of identifying cancer and clarifying the benign or malignant nature of findings seen on anatomic imaging—as is the case in the application of FDG PET to pulmonary nodules detected by CT.<sup>118</sup> Since HP MRI is readily coupled to the anatomic information acquired from standard MRI, it may also be particularly helpful in directing tissue sampling by identifying the sites most suspicious for cancer or, in the case of large cancer or widespread lesions, indicating the lesions that appear most aggressive. Finally, HP MRI could play a role in stratifying tumors identified by other imaging modalities. Also, the application of HP MRI for systemic staging is unlikely in the short term as it would require a whole-body capability similar to that of PET/CT, the development of which would have to overcome several technical challenges. However, as discussed above, these technical challenges are beginning to be addressed in ongoing phase II clinical trials of metastatic cancer.

Our understanding of cancer metabolism is primarily based on cell and murine models whose relevance to human malignancies is unclear. Consequently, in addition to the traditional roles of imaging in cancer management, HP MRI could provide clinical value based on its capacity to identify specific therapeutic targets *in vivo* in humans, i.e., serve as companion diagnostics. Accordingly, the presence of accelerated lactate production could direct the use of LDH inhibitors, while altered mitochondrial metabolism might suggest therapeutic options to renormalize metabolic activity.

#### How Could HP Information Change a Therapeutic Decision?

Since the publication of the first white paper,<sup>3</sup> a number of reports have appeared on the evaluation of cancer biomarkers and cancer imaging methods.<sup>114,117,119–122</sup> HP <sup>13</sup>C MRI holds great promise as an imaging biomarker of cancer. An imaging biomarker has been defined as an anatomic, biochemical, or molecular parameter detectable with an imaging method that is useful for establishing the presence or severity of disease.<sup>123,124</sup> As we have already mentioned, metabolic alteration is an important phenotypic feature of cancer that predicts disease behavior and can itself be a therapeutic target.<sup>121,125</sup> A critical consideration in the translation of a new biomarker into the clinic is the impact of the test necessary for obtaining this biomarker on clinical practice and patient outcome.<sup>119</sup> In other words, does the test lead to better, more effective, and/or more cost-effective patient treatment? As a cancer molecular imaging biomarker, HP <sup>13</sup>C MRI has the potential to address the following five clinical needs.<sup>115</sup>

First, HP MRI could prove beneficial by detecting disease prior to its initial clinical manifestation—in high-risk patients, for example—or as a secondary diagnostic test, indicating the likelihood that abnormal findings from screening or staging studies represent a malignancy. It could also prove valuable by helping to stratify disease severity after a diagnosis. Second, HP MRI could identify specific sites for tissue biopsy for cancer diagnosis and characterization. A third important benefit would be the capacity to predict disease progression based on evidence of metabolic hyperactivity or the integrity of metabolic pathways that enable metastasis. Fourth, HP MRI may provide an early, pharmacodynamic measure of drug efficacy, which could in turn predict the likelihood of therapeutic futility, by measuring the impact of a given drug on regional cancer

metabolism. If validated, this would be a significant clinical contribution, as it would enable the avoidance of ineffective chemotherapy with the attendant morbidity and expense. Finally, HP MRI could prove useful in evaluating prognosis and indicating overall response—using the eradication of aberrant metabolism as a highly predictive indicator of disease resolution, akin to the use of FDG PET/CT in lymphoma.<sup>126</sup> In this context, the role of HP would be to determine whether or not treatment has eliminated the cancer, as well as to help determine if there is a need for additional treatment by predicting the likelihood of disease relapse or progression. In summary, biomarker applications are likely to represent the most compelling use of HP <sup>13</sup>C MRI in relation to cancer since its unique ability to characterize and quantify cancer metabolism provides a means for inferring the impact of targeted therapeutic interventions.<sup>122,127</sup>

### *What Will a Clinician Look for in Studies of HP Validation?*

Experience with cancer diagnostics<sup>119,120</sup> suggests that the general term “validation” may refer to distinct criteria: validity with respect to analytical results, validity for the purpose of a clinical diagnosis, and validity for the purpose of modifying patient care, which could also be termed clinical utility. In order to support the use of HP <sup>13</sup>C MRI in clinical trials and clinical practice, investigations relevant to all three classes of data will be needed.

Analytic validity will be an important question, as clinicians will need to understand what HP <sup>13</sup>C MRI is measuring and see evidence that these measurements are accurate. One approach to establishing the analytic validity of HP MRI is to compare its results with those of other PET-based tracer experiments. Demonstrating the reproducibility of hyperpolarized imaging exams is another important step and will require establishing standardized and repeatable methods for HP MR image acquisition and interpretation. Clinical validity, on the other hand, refers to the capacity of a test to separate a given patient population into two groups, such as those with and without a disease. To establish their clinical validity, HP MRI results must be compared to an accepted clinical standard such as the tissue or laboratory-based assays with which oncologists are most comfortable. Another important aspect of demonstrating HP MRI's clinical validity will be its comparison to FDG and other PET imaging methods, and for this reason, investment in facilities capable of performing both exams is critical.

It is important to acknowledge, however, that establishing the clinical validity of a given technology does not in and of itself demonstrate that this technology should be used in patient care decisions. Rather, that determination is ultimately based on clinical utility, which refers to the technology's capacity to appropriately direct patient care. In assessing the clinical utility of HP <sup>13</sup>C MRI, clinicians will look for validation against clinical outcomes, accuracy (sensitivity, specificity, receiver operating characteristic area) versus a reference standard in diagnostic applications, and predictive accuracy in assessing therapeutic response. It will therefore be important to know to what extent the data provided by HP MRI accurately reclassify a patient, after all conventional studies are complete, into the proper category—classified either as normal (with a normal HP exam) or as disease (with an abnormal HP exam). Additional criteria will include the risk or discomfort of the exam relative to the new information it provides and, of course, the cost. Utility will be a key component of later clinical trials, in which assessment of the impact on patient outcomes and the cost of medical care provide data for

coverage decisions by payers, which is one of the most important determinants of whether or not a new test is actually used in the clinic.<sup>119</sup>

### *Comparison to Positron Tomography*

Lessons learned from other quantitative molecular methods such as PET can help guide the approach to quantitative image analysis using HP MRI. For example, studies have shown that more sophisticated quantitative methods such as compartmental kinetic analysis can improve the ability to measure therapeutic response and predict patient outcomes<sup>128</sup>; however, this improvement must be balanced against the ability to implement more complex methods in the clinic.<sup>129</sup> Experience suggests that necessary simplification is best achieved by collecting detailed data in early studies and then testing the impact of simplification against more rigorous analytic approaches.<sup>130</sup>

Combining HP MRI and PET data in kinetic analysis may be especially powerful in characterizing cancer metabolism, as the two methods provide complementary information. Long half-life and relatively straightforward image quantification make PET a robust method for quantifying flux through certain specific biochemical pathways, such as the flux of glucose through hexokinases as a measure of glycolysis or of thymidine through TK as a measure of cellular proliferation. However, since isotopic emissions are not impacted by the chemical species to which the isotope is attached, PET provides no information about the nature of the molecule attached to the label. HP <sup>13</sup>C MRI, on the other hand, provides exquisite information on the evaluation of metabolites of the injected substance—such as for lactate from pyruvate—while its shorter half-life makes studies of metabolic trapping difficult. Taken together, the two methods can provide comprehensive information on metabolic fluxes, especially at major branch points in metabolic pathways such as the conversion of pyruvate to lactate in glycolysis.

### *Future Directions: Initial Studies and Clinical Study Design*

*Early Clinical Trials.* Existing guidelines for designing and reporting on clinical trials of biomarkers provide a helpful template for HP <sup>13</sup>C MRI.<sup>131</sup> Early studies must refine and test robust methods for image acquisition and analysis to provide a uniform (and uniformly accepted) approach to be used in subsequent clinical trials. Early studies should also include tests of repeatability/precision to measure the qualitative and quantitative variability of HP imaging results, typically using a test/retest paradigm.<sup>113</sup> Guidelines based on results from early clinical trials are important for subsequent trials and eventual clinical use, as the NCI consensus guidelines on FDG PET/CT have demonstrated.<sup>132</sup> Finally, early clinical trials should validate HP <sup>13</sup>C MRI against an accepted reference standard for cancer diagnosis and characterization, typically based on tissue sampling. This reference standard can be the presence or absence of cancer for diagnostic applications, or specific assays that might serve as a reference for imaging measures and which are often established in preclinical studies. In addition to standardizing imaging approaches, reporting of adverse events also could be standardized to facilitate regulatory approval down the road.

The latter phase of imaging trials for biomarker applications should evaluate new imaging tests for their accuracy in predicting important clinical cancer outcomes such as therapeutic response, progression-free survival, and overall survival. Early studies must establish the

value in clinical trials of HP  $^{13}\text{C}$  MRI as integrated markers, where novel imaging is embedded in a clinical trial but is collected in a purely observational fashion for comparison against clinical outcomes measured in the treatment trial.<sup>133</sup> Once validated in integral biomarker trials, the imaging marker can be used to direct therapy in a clinical trial and, later, in clinical practice. An example can again be found in the application of FDG PET/CT to lymphoma, where the resolution of abnormal FDG uptake, known as a complete metabolic response, was shown to be highly predictive of disease-free survival and is now used as an integral marker in clinical trials and for clinical practice.<sup>126</sup>

**Multisite Trials.** Multisite clinical trials will be expected prior to FDA approval of  $[1-^{13}\text{C}]$ pyruvate as an imaging agent, and certain specific obstacles will have to be addressed in designing them. In addition to requiring novel imaging hardware, acquisition methods, and analysis, HP  $^{13}\text{C}$  MRI carries the added challenge of requiring the administration of a short-lived, locally produced imaging probe, the production of which requires onsite personnel with expertise in producing HP agents, monitoring their quality, and assuring patient safety and regulatory compliance. The ability to produce uniformly high-quality HP imaging agents across multiple centers is therefore a crucial step in moving to multicenter clinical trials and eventual clinical practice. Once again, some lessons can be learned from recent multisite tests of investigational PET probes, which share many of these requirements.<sup>134,135</sup> The foremost requirement is that of validated, uniform standards for probe production that will support equivalent probe quality across all sites involved participating in multicenter trials. This allows operation under a common regulatory framework—for example, an NCI-held IND<sup>136</sup> for multicenter clinical trials—and assures patient safety and consistency of the drug product. Standardized, robust image acquisition methods are also needed, as are methods for testing and qualifying equipment and personnel involved in HP MRI studies to ensure high-quality imaging data at all participating sites.

Experience suggests a multistep approach leading to multicenter trials for novel imaging approaches such as MRI of HP  $[1-^{13}\text{C}]$  pyruvate<sup>119</sup> will be key for obtaining full FDA approval. Early studies to test the potential accuracy and utility of new imaging methods are often best done in single-center studies at expert institutions invested in the technology. Early multicenter phase II trials should be small enough to assure the ability of sites to acquire the imaging data in a uniform and reproducible fashion and should validate the findings from single-center trials; indications supported by small multicenter trials can then be carried into larger phase III studies using well-defined, prospective procedures for image analysis, with study design and sample size calculations guided by results from smaller multisite or single-site trials. Larger phase II trials should include endpoints for safety and efficacy—in this case defined as diagnostic accuracy. These larger studies should also gather information on therapeutic impact and cost-effectiveness, key data for coverage decisions by the Center for Medicare and Medicaid Services and other payers.

### Education, Training, and Certification

In addition to regulatory approval, translation to clinical practice will require training for staff members who produce HP probes and carry out HP  $^{13}\text{C}$  MR imaging. Imaging physicians will also need to be trained in this new imaging modality: not only how to interpret the data it provides but also how to safely and effectively administer HP imaging probes. Experience with other highly specialized imaging

methods such as PET and breast MRI<sup>137,138</sup> suggests that requirements for physician training and certification will be important in assuring uniform diagnostic quality across all sites of practice. Finally, even after clinical practice implementation, ongoing clinical research will be critical for sustaining and optimizing clinical use.

### Recommendations for Future Research

Since the publication of the first NIH white paper on hyperpolarized  $^{13}\text{C}$  MRI in 2011, numerous preclinical studies have demonstrated this technology's unique metabolic imaging capabilities in the context of cancer. There have now been over 200 HP  $^{13}\text{C}$  MRI human studies performed to date worldwide at 7 different medical centers, and over 5 more sites plan to initiate patient studies within the next 6 months. All of these studies have shown that HP  $^{13}\text{C}$  pyruvate MRI is safe and also effective in detecting key metabolic conversions in patients with a variety of diseases and even in normal volunteers. It is important to recognize that demonstrating the clinical safety and feasibility of HP MRI technology is not enough to ensure its widespread clinical implementation. If the latter is to be achieved, it will be because future trials are able to successfully establish its *clinical utility*. In addition, widespread clinical implementation also implies regulatory approval and reimbursement approvals around the world. Commercialization of HP  $[1-^{13}\text{C}]$ pyruvate MRI will require a comprehensive regulatory and sponsorship strategy that will also depend on the potential clinical utility. We have developed a number of recommendations with this ultimate goal in mind.

First, it is necessary to continue refining the protocols, new HP agents, and investigative targets of ongoing preclinical studies in a translational direction with refined pharmacy methods for reliable, lower-cost production of sterile HP solutions. Also, it is valuable to verify that metabolic measurements in animal models of cancer and other disease states correspond to those performed in human disease, and to incorporate these measurements into disease hypothesis testing and development of new hyperpolarized agents. Improved quantitative analysis of metabolite signals and enzymatic rate kinetics obtained from HP  $[1-^{13}\text{C}]$  pyruvate will be a critical aspect of this. It is also imperative to identify the metabolic network(s) associated with the metabolism of specific hyperpolarized agents in order to select the appropriate agent for the study of specific disease conditions and therapies, and to appropriately guard against incorrectly associating apparent metabolic changes with the wrong cause. Additionally, there is a need for more studies which focus on determining the origins of variability in therapeutic response through separate HP measures of uptake and metabolism, and to use these HP probes to identify and better understand therapeutic response and nonresponders at earlier time points.

Further efforts to develop improved imaging pulse sequences and RF coils for imaging different organs, agents, and disease states will be critical for increased quality, information content, and applicability. New RF hardware should enable body-coil transmit and multichannel (32 at least) reception for all parts of the body with both  $^{13}\text{C}$  and  $^1\text{H}$  frequency excitation and reception. Analysis methods for the reliable calculation of enzymatic rate constants, such as  $k_{\text{PL}}$  for the LDH catalyzed conversion of pyruvate to lactate and  $k_{\text{PB}}$  for pyruvate to bicarbonate, need to be refined and tested in patient and volunteer studies at multiple sites. In the context of cancer more specifically, another vital avenue for future studies will be the development of new HP agents capable of probing the ancillary and often-unexpected metabolic changes leading to increased cancer cell survival after

therapy. Specialized MR pulse sequences for the new agents will be required and  $^1\text{H}$  detected- $^{13}\text{C}$  spectroscopy techniques should be developed and investigated for increased sensitivity with the added advantage that spatial information can be encoded at the  $^1\text{H}$  frequency.

There are also a number of needs to be addressed at an institutional level. First and foremost, the mechanism(s) for multisite clinical trials must be established—both through the identification of sites that possess the necessary equipment and by developing the appropriate investigative protocols. In order to support these efforts, it is important to promote the development of pedagogical resources for real-time metabolic imaging, perhaps through the establishment of new pre- and postdoctoral training programs focused on developing relevant techniques.

Finally, widespread clinical translation will not be possible without the continued development of robust collaborations among basic science investigators, clinical oncologists, and those with expertise in clinical study design. This collaborative work must be bolstered by strong partnerships between academia, funding agencies, and industry.

### Acknowledgements

This report was initiated through discussions with representatives of the NCI Cancer Imaging Program and other NIH extramural programs (National Institute of Diabetes and Digestive and Kidney Diseases; National Heart, Lung, and Blood Institute; National Institute of Biomedical Imaging and Bioengineering; and NIH Research Infrastructure Programs). The initial draft was reviewed and edited by over 60 scientists, followed by extensive discussions at a workshop at the ISMRM meeting in May 2017 with more than 52 scientists from academia, industry, and federal agencies from the United States and other countries. The authors appreciate the assistance from NIH extramural program staff Drs. Huiming Zhang, Maren Laughlin, Guoying Liu, Larry Clarke, Paula Jacobs, Janet Eary, and Lalitha Shankar during the development of this report and for organizing the workshop. The authors would also like to thank other contributors, namely, Drs. Michael Boss and Karl Stupic from NIST, Dr. Murali C Krishna from NCI intramural, and Dr. Matthew G. Vander Heiden from MIT.

### References

- [1] Cairns RA, Harris IS, and Mak TW (2011). Regulation of cancer cell metabolism. *Nat Rev Cancer* **11**, 85–95. <https://doi.org/10.1038/nrc2981>.
- [2] Timm KN, Kennedy BWC, and Brindle KM (2016). Imaging tumor metabolism to assess disease progression and treatment response. *Clin Cancer Res* **22**, 5196–5203. <https://doi.org/10.1158/1078-0432.CCR-16-0159>.
- [3] J. Kurhanewicz, D. B. Vigneron, K. Brindle, E. Y. Chekmenev, A. Comment, C. H. Cunningham, R. J. Deberardinis, G. G. Green, M. O. Leach, S. S. Rajan, et al.
- [4] Tee S-S and Keshari KR (2015). Novel approaches to imaging tumor metabolism. *Cancer J* **21**, 165–173. <https://doi.org/10.1097/PPO.0000000000000111>.
- [5] Siddiqui S, Kadlecak S, Pourfathi M, Xin Y, Mannherz W, Hamedani H, Drachman N, Ruppert K, Clapp J, and Rizi R (2017). The use of hyperpolarized carbon-13 magnetic resonance for molecular imaging. *Adv Drug Deliv Rev* **113**, 3.
- [6] Zhang H (2014). The potential of hyperpolarized  $^{13}\text{C}$  MRI in assessing signaling pathways in cancer. *Acad Radiol* **21**, 215–222. <https://doi.org/10.1016/j.acra.2013.11.015>.
- [7] Bowers CR and Weitekamp DP (1987). Parahydrogen and synthesis allow dramatically enhanced nuclear alignment. *J Am Chem Soc* **109**, 5541–5542. <https://doi.org/10.1021/ja00252a049>.

- [8] P. Bhattacharya, E. Y. Chekmenev, W. F. Reynolds, S. Wagner, N. Zacharias, H. R. Chan, R. Bunger, B. D. Ross, Parahydrogen-induced polarization (PHIP) hyperpolarized MR receptor imaging in vivo: a pilot study of  $^{13}\text{C}$  imaging of atheroma in mice. *NMR Biomed* **24**, 1023.
- [9] Walker TG and Happer W (1997). Spin-exchange optical pumping of noble-gas nuclei. *Rev Mod Phys* **69**, 629–642. <https://doi.org/10.1103/RevModPhys.69.629>.
- [10] Mugler JP, Altes TA, Ruset IC, Dregely IM, Mata JF, and Miller GW, et al (2010). Simultaneous magnetic resonance imaging of ventilation distribution and gas uptake in the human lung using hyperpolarized xenon-129. *PNAS* **107**, 21707–21712. <https://doi.org/10.1073/pnas.1011912107>.
- [11] Gabellieri C, Reynolds S, Lavie A, Payne GS, Leach MO, and Eykyn TR (2008). Therapeutic target metabolism observed using hyperpolarized  $^{15}\text{N}$  choline. *J Am Chem Soc* **130**, 4598–4599. <https://doi.org/10.1021/ja8001293>.
- [12] Hu S, Balakrishnan A, Bok RA, Anderton B, Larson PEZ, and Nelson SJ, et al (2011).  $^{13}\text{C}$ -pyruvate imaging reveals alterations in glycolysis that precede c-Myc-induced tumor formation and regression. *Cell Metab* **14**, 131–142. <https://doi.org/10.1016/j.cmet.2011.04.012>.
- [13] Keshari KR, Sriram R, Van Criekinge M, Wilson DM, Wang ZJ, and Vigneron DB, et al (2013). Metabolic reprogramming and validation of hyperpolarized  $^{13}\text{C}$  lactate as a prostate cancer biomarker using a human prostate tissue slice culture bioreactor. *Prostate* **73**, 1171–1181. <https://doi.org/10.1002/pros.22665>.
- [14] Sriram R, Van Criekinge M, DeLos Santos J, Keshari KR, Wilson DM, Peehl D, Kurhanewicz J, and Wang ZJ (2016). Non-invasive differentiation of benign renal tumors from clear cell renal cell carcinomas using clinically translatable hyperpolarized ( $^{13}\text{C}$ ) pyruvate magnetic resonance. *Tomography* **2**, 35.
- [15] Sriram R, Van Criekinge M, Hansen A, Wang ZJ, Vigneron DB, Wilson DM, Keshari KR, and Kurhanewicz J (2015). Real-time measurement of hyperpolarized lactate production and efflux as a biomarker of tumor aggressiveness in an MR compatible 3D cell culture bioreactor. *NMR Biomed* **28**, 1141.
- [16] Rajeshkumar NV, Dutta P, Yabuuchi S, de Wilde RF, Martinez GV, Le A, Kamphorst JJ, Rabinowitz JD, Jain SK, and Hidalgo M, et al (2015). Therapeutic targeting of the Warburg effect in pancreatic cancer relies on an absence of p53 function. *Cancer Res* **75**, 3355.
- [17] Viswanath P, Najac C, Izquierdo-Garcia JL, Pankov A, Hong C, Eriksson P, Costello JF, Pieper RO, and Ronen SM (2016). Mutant IDH1 expression is associated with down-regulation of monocarboxylate transporters. *Oncotarget* **7**, 34942.
- [18] Day SE, Kettunen MI, Gallagher FA, Hu DE, Lerche M, Wolber J, Golman K, Ardenkjaer-Larsen JH, and Brindle KM (2007). Detecting tumor response to treatment using hyperpolarized  $^{13}\text{C}$  magnetic resonance imaging and spectroscopy. *Nat Med* **13**, 1382.
- [19] Izquierdo-Garcia JL, Viswanath P, Eriksson P, Cai L, Radoul M, Chaumeil MM, Blough M, Luchman HA, Weiss S, and Cairncross JG, et al (2015). IDH1 Mutation induces reprogramming of pyruvate metabolism. *Cancer Res* **75**, 2999.
- [20] Park JM, Spielman DM, Josan S, Jang T, Merchant M, Hurd RE, Mayer D, and Recht LD (2016). Hyperpolarized ( $^{13}\text{C}$ )-lactate to ( $^{13}\text{C}$ )-bicarbonate ratio as a biomarker for monitoring the acute response of anti-vascular endothelial growth factor (anti-VEGF) treatment. *NMR Biomed* **29**, 650.
- [21] Saito K, Matsumoto S, Takakusagi Y, Matsuo M, Morris HD, Lizak MJ, Munasinghe JP, Devasahayam N, Subramanian S, and Mitchell JB, et al (2015).  $^{13}\text{C}$ -MR Spectroscopic imaging with hyperpolarized [ $1-^{13}\text{C}$ ]pyruvate detects early response to radiotherapy in SCC tumors and HT-29 tumors. *Clin Cancer Res* **21**, 5073.
- [22] Wojtkowiak JW, Cornnell HC, Matsumoto S, Saito K, Takakusagi Y, Dutta P, Kim M, Zhang X, Leos R, and Bailey KM, et al (2015). Pyruvate sensitizes pancreatic tumors to hypoxia-activated prodrug TH-302. *Cancer Metab* **3**, 2.
- [23] Park I, Mukherjee J, Ito M, Chaumeil MM, Jalbert LE, Gaensler K, Ronen SM, Nelson SJ, and Pieper RO (2014). Changes in pyruvate metabolism detected by magnetic resonance imaging are linked to DNA damage and serve as a sensor of temozolomide response in glioblastoma cells. *Cancer Res* **74**, 7115.
- [24] Sandulache VC, Chen Y, Lee J, Rubinstein A, Ramirez MS, Skinner HD, Walker CM, Williams MD, Taylor R, and Court LE, et al (2014). Evaluation of hyperpolarized [ $1-(1)^{13}\text{C}$ ]-pyruvate by magnetic resonance to detect ionizing radiation effects in real time. *PLoS One* **9**, e87031.

- [25] Asghar Butt S, Sogaard LV, Ardenkjaer-Larsen JH, Lauritzen MH, Engelholm LH, Paulson OB, Mirza O, Holck S, Magnusson P, and Akeson P (2015). Monitoring mammary tumor progression and effect of tamoxifen treatment in MMTV-PyMT using MRI and magnetic resonance spectroscopy with hyperpolarized [1-<sup>13</sup>C]pyruvate. *Magn Reson Med* **73**, 51.
- [26] Dutta P, Le A, Vander Jagt DL, Tsukamoto T, Martinez GV, Dang CV, and Gillies RJ (2013). Evaluation of LDH-A and glutaminase inhibition in vivo by hyperpolarized <sup>13</sup>C-pyruvate magnetic resonance spectroscopy of tumors. *Cancer Res* **73**, 4190.
- [27] Chen AP, Chu W, Gu Y-P, Cunningham CH, and Cunningham CH (2013). Probing early tumor response to radiation therapy using hyperpolarized [1-<sup>13</sup>C] pyruvate in MDA-MB-231 xenografts. *PLoS One* **8**e56551. <https://doi.org/10.1371/journal.pone.0056551>.
- [28] Park JM, Recht LD, Josan S, Merchant M, Jang T, Yen YF, Hurd RE, Spielman DM, and Mayer D (2013). Metabolic response of glioma to dichloroacetate measured in vivo by hyperpolarized (<sup>13</sup>C) magnetic resonance spectroscopic imaging. *Neuro-Oncology* **15**, 433.
- [29] Lodi A, Woods SM, and Ronen SM (2013). Treatment with the MEK inhibitor U0126 induces decreased hyperpolarized pyruvate to lactate conversion in breast, but not prostate, cancer cells. *NMR Biomed* **26**, 299–306. <https://doi.org/10.1002/nbm.2848>.
- [30] Radoul M, Chaumeil MM, Eriksson P, Wang AS, Phillips JJ, and Ronen SM (2016). MR Studies of glioblastoma models treated with Dual PI3K/mTOR inhibitor and temozolomide: metabolic changes are associated with enhanced survival. *Mol Cancer Ther* **15**, 1113–1122. <https://doi.org/10.1158/1535-7163.MCT-15-0769>.
- [31] Bohndiek SE, Kettunen MI, Hu DE, and Brindle KM (2012). Hyperpolarized <sup>13</sup>C spectroscopy detects early changes in tumor vasculature and metabolism after VEGF neutralization. *Cancer Res* **72**, 854–864. <https://doi.org/10.1158/0008-5472.CAN-11-2795>.
- [32] Chaumeil MM, Ozawa T, Park I, Scott K, James CD, Nelson SJ, and Ronen SM (2012). Hyperpolarized <sup>13</sup>C MR spectroscopic imaging can be used to monitor everolimus treatment in vivo in an orthotopic rodent model of glioblastoma. *NeuroImage* **59**, 193.
- [33] Duwel S, Durst M, Gringeri CV, Kosanke Y, Gross C, Janich MA, Haase A, Glaser SJ, Schwaiger M, and Schulte RF, et al (2016). Multiparametric human hepatocellular carcinoma characterization and therapy response evaluation by hyperpolarized (<sup>13</sup>C) MRSI. *NMR Biomed* **29**, 952.
- [34] Nelson SJ, Kurhanewicz J, Vigneron DB, Larson PE, Harzstark AL, Ferrone M, van Criekinge M, Chang JW, Bok R, and Park I, et al (2013). Metabolic imaging of patients with prostate cancer using hyperpolarized [1-(1<sup>3</sup>C)] pyruvate. *Sci Transl Med* **5**198ra108.
- [35] Keshari KR, Sriram R, Koelsch BL, Van Criekinge M, Wilson DM, Kurhanewicz J, and Wang ZJ (2013). Hyperpolarized <sup>13</sup>C-pyruvate magnetic resonance reveals rapid lactate export in metastatic renal cell carcinomas. *Cancer Res* **73**, 529.
- [36] Keshari KR, Wilson DM, Van Criekinge M, Sriram R, Koelsch BL, Wang ZJ, VanBrocklin HF, Pechl DM, O'Brien T, and Sampath D, et al (2015). Metabolic response of prostate cancer to nicotinamide phosphoribosyltransferase inhibition in a hyperpolarized MR/PET compatible bioreactor. *Prostate* **75**, 1601.
- [37] Xu HN, Kadlecsek S, Profka H, Glickson JD, Rizi R, and Li LZ (2014). Is higher lactate an indicator of tumor metastatic risk? A pilot MRS study using hyperpolarized (<sup>13</sup>C)-pyruvate. *Acad Radiol* **21**, 223–231. <https://doi.org/10.1016/j.acra.2013.11.014>.
- [38] Chaumeil MM, Radoul M, Najac C, Eriksson P, Viswanath P, Blough MD, Chesnelong C, Luchman HA, Cairncross JG, and Ronen SM (2016). Hyperpolarized (<sup>13</sup>C) MR imaging detects no lactate production in mutant IDH1 gliomas: Implications for diagnosis and response monitoring. *Neuro-Image Clin* **12**, 180.
- [39] Sandulache VC, Skinner HD, Wang Y, Chen Y, Dodge CT, Ow TJ, Bankson JA, Myers JN, and Lai SY (2012). Glycolytic inhibition alters anaplastic thyroid carcinoma tumor metabolism and improves response to conventional chemotherapy and radiation. *Mol Cancer Ther* **11**, 1373.
- [40] Venkatanarayan A, Raulji P, Norton W, Chakravarti D, Coarfa C, Su X, Sandur SK, Ramirez MS, Lee J, and Kingsley CV, et al (2015). IAPP-driven metabolic reprogramming induces regression of p53-deficient tumours in vivo. *Nature* **517**, 626.
- [41] Phan L, Chou PC, Velazquez-Torres G, Samudio I, Parreno K, Huang Y, Tseng C, Vu T, Gully C, and Su CH, et al (2015). The cell cycle regulator 14-3-3sigma opposes and reverses cancer metabolic reprogramming. *Nat Commun* **6**, 7530.
- [42] Jeong S, Eskandari R, Park SM, Alvarez J, Tee SS, Weissleder R, Kharas MG, Lee H, and Keshari KR (2017). Real-time quantitative analysis of metabolic flux in live cells using a hyperpolarized micromagnetic resonance spectrometer. *Sci Adv* **3**e1700341.
- [43] Albers MJ, Bok R, Chen AP, Cunningham CH, Zierhut ML, Zhang VY, Kohler SJ, Tropp J, Hurd RE, and Yen YF, et al (2008). Hyperpolarized <sup>13</sup>C lactate, pyruvate, and alanine: noninvasive biomarkers for prostate cancer detection and grading. *Cancer Res* **68**, 8607.
- [44] Serrao EM, Kettunen MI, Rodrigues TB, Dzien P, Wright AJ, Gopinathan A, Gallagher FA, Lewis DY, Frese KK, and Almeida J, et al (2016). MRI with hyperpolarized [1-<sup>13</sup>C]pyruvate detects advanced pancreatic preneoplasia prior to invasive disease in a mouse model. *Gut* **65**, 465.
- [45] Bard-Chapeau EA, Nguyen AT, Rust AG, Sayadi A, Lee P, Chua BQ, New LS, de Jong J, Ward JM, and Chin CK, et al (2014). Transposon mutagenesis identifies genes driving hepatocellular carcinoma in a chronic hepatitis B mouse model. *Nat Genet* **46**, 24.
- [46] Gutte H, Hansen AE, Larsen MM, Rahbek S, Henriksen ST, Johannesen HH, Ardenkjaer-Larsen J, Kristensen AT, Hojgaard L, and Kjaer A (2015). Simultaneous hyperpolarized <sup>13</sup>C-pyruvate MRI and <sup>18</sup>F-FDG PET (HyperPET) in 10 dogs with cancer. *J Nucl Med* **56**, 1786.
- [47] Gutte H, Hansen AE, Henriksen ST, Johannesen HH, Ardenkjaer-Larsen J, Vignaud A, Hansen AE, Borresen B, Klausen TL, and Wittekind AM, et al (2015). Simultaneous hyperpolarized (<sup>13</sup>C)-pyruvate MRI and (<sup>18</sup>F)-FDG-PET in cancer (hyperPET): feasibility of a new imaging concept using a clinical PET/MRI scanner. *Am J Nucl Med Mol Imaging* **5**, 38.
- [48] Mignon L, Dutta P, Martinez GV, Foroutan P, Gillies RJ, and Jordan BF (2014). Monitoring chemotherapeutic response by hyperpolarized <sup>13</sup>C-fumarate MRS and diffusion MRI. *Cancer Res* **74**, 686–694. <https://doi.org/10.1158/0008-5472.CAN-13-1914>.
- [49] Gehan EA and Tefft MC (2000). Will there be resistance to the RECIST (Response Evaluation Criteria in Solid Tumors)? *J Natl Cancer Inst* **92**, 179–181.
- [50] Golman K, in 't Zandt R, and Thaning M (2006). Real-time metabolic imaging. *PNAS* **103**, 11270–11275. <https://doi.org/10.1073/pnas.0601319103>.
- [51] Keshari KR and Wilson DM (2014). Chemistry and biochemistry of <sup>13</sup>C hyperpolarized magnetic resonance using dynamic nuclear polarization. *Chem Soc Rev* **43**, 1627–1659. <https://doi.org/10.1039/c3cs60124b>.
- [52] Bastiaansen JAM, Cheng T, Mishkovsky M, Duarte JMN, Comment A, and Gruetter R (1830). In vivo enzymatic activity of acetylCoA synthetase in skeletal muscle revealed by (<sup>13</sup>C) turnover from hyperpolarized [1-(<sup>13</sup>C)]acetate to [1-(<sup>13</sup>C)]acetylarnitine. *Biochim Biophys Acta* **2013**, 4171–4178. <https://doi.org/10.1016/j.bbagen.2013.03.023>.
- [53] Flori A, Liserani M, Frijia F, Giovannetti G, Lionetti V, Casieri V, Positano V, Aquaro GD, Recchia FA, and Santarelli MF, et al (2015). Real-time cardiac metabolism assessed with hyperpolarized [1-(<sup>13</sup>C)]acetate in a large-animal model. *Contrast Media Mol Imaging* **10**, 194.
- [54] Ball DR, Rowlands B, Dodd MS, Le Page L, Ball V, Carr CA, Clarke K, and Tyler DJ (2014). Hyperpolarized butyrate: a metabolic probe of short chain fatty acid metabolism in the heart. *Magn Reson Med* **71**, 1663.
- [55] Hu S, Zhu M, Yoshihara HA, Wilson DM, Keshari KR, Shin P, Reed G, von Morze C, Bok R, and Larson PE, et al (2011). In vivo measurement of normal rat intracellular pyruvate and lactate levels after injection of hyperpolarized [1-(<sup>13</sup>C)]alanine. *Magn Reson Imaging* **29**, 1035.
- [56] Felig P (1973). The glucose-alanine cycle. *Metabolism* **22**, 179–207. [https://doi.org/10.1016/0026-0495\(73\)90269-2](https://doi.org/10.1016/0026-0495(73)90269-2).
- [57] Rodrigues TB, Serrao EM, Kennedy BWC, Hu D, Kettunen MI, and Brindle KM (2014). Magnetic resonance imaging of tumor glycolysis using hyperpolarized <sup>13</sup>C-labeled glucose. *Nat Med* **20**. <https://doi.org/10.1038/nm.3416>.
- [58] Harris T, Degani H, and Frydman L (2013). Hyperpolarized <sup>13</sup>C NMR studies of glucose metabolism in living breast cancer cell cultures. *NMR Biomed* **26**, 1831–1843. <https://doi.org/10.1002/nbm.3024>.
- [59] Keshari KR, Kurhanewicz J, Bok R, Larson PEZ, Vigneron DB, and Wilson DM (2011). Hyperpolarized <sup>13</sup>C dehydroascorbate as an endogenous redox sensor for in vivo metabolic imaging. *Proc Natl Acad Sci U S A* **108**, 18606–18611. <https://doi.org/10.1073/pnas.1106920108>.
- [60] Bohndiek SE, Kettunen MI, Hu DE, Kennedy BW, Boren J, Gallagher FA, and Brindle KM (2011). Hyperpolarized [1-<sup>13</sup>C]-ascorbic and dehydroascorbic

- acid: vitamin C as a probe for imaging redox status in vivo. *J Am Chem Soc* **133**:11795.
- [61] Timm KN, Hu DE, Williams M, Wright AJ, Kettunen MI, Kennedy BW, Larkin TJ, Dzien P, Marco-Rius I, and Bohndiek SE, et al (2017). Assessing oxidative stress in tumors by measuring the rate of hyperpolarized [1-13C] dehydroascorbic acid reduction using 13C magnetic resonance spectroscopy. *J Biol Chem* **292**, 1737.
- [62] Chaumeil MM, Larson PE, Woods SM, Cai L, Eriksson P, Robinson AE, Lupo JM, Vigneron DB, Nelson SJ, and Pieper RO, et al (2014). Hyperpolarized [1-13C] glutamate: a metabolic imaging biomarker of IDH1 mutational status in glioma. *Cancer Res* **74**, 4247.
- [63] Chaumeil MM, Larson PE, Yoshihara HA, Danforth OM, Vigneron DB, Nelson SJ, Pieper RO, Phillips JJ, and Ronen SM (2013). Non-invasive in vivo assessment of IDH1 mutational status in glioma. *Nat Commun* **4**, 2429.
- [64] Salamanca-Cardona L, Shah H, Poot AJ, Correa FM, Di Gialleonardo V, Lui H, Miloushev VZ, Granlund KL, Tee SS, and Cross JR, et al (2017). In vivo imaging of glutamine metabolism to the oncometabolite 2-hydroxyglutarate in IDH1/2 mutant tumors. *Cell Metab* **26**, 830.
- [65] Moreno KX, Satapati S, DeBerardinis RJ, Burgess SC, Malloy CR, and Merritt ME (2014). Real-time detection of hepatic gluconeogenic and glycogenolytic states using hyperpolarized [2-13C]dihydroxyacetone. *J Biol Chem* **289**, 35859–35867. <https://doi.org/10.1074/jbc.M114.613265>.
- [66] Chen W, Khemtong C, Jiang W, Malloy CR, and Sherry AD (2016). Metabolism of Hyperpolarized 13C-Acetoacetate/ $\beta$ -Hydroxybutyrate Reveals Mitochondrial Redox State in Perfused Rat Hearts. Presented at the ISMRM 24th Annual Meeting, Singapore; 2016.
- [67] von Morze C, Bok RA, Reed GD, Ardenkjaer-Larsen JH, Kurhanewicz J, and Vigneron DB (2014). Simultaneous multiagent hyperpolarized (13)C perfusion imaging. *Magn Reson Med* **72**, 1599–1609. <https://doi.org/10.1002/mrm.25071>.
- [68] Lau AZ, Miller JJ, Robson MD, and Tyler DJ (2016). Simultaneous assessment of cardiac metabolism and perfusion using copolarized [1-(13)C]pyruvate and (13)C-urea. *Magn Reson Med*. <https://doi.org/10.1002/mrm.26106>.
- [69] Bankson JA, Walker CM, Ramirez MS, Stefan W, Fuentes D, Merritt ME, Lee J, Sandulache VC, Chen Y, and Phan L, et al (2015). Kinetic modeling and constrained reconstruction of hyperpolarized [1-13C]-pyruvate offers improved metabolic imaging of tumors. *Cancer Res* **75**, 4708.
- [70] Bohndiek SE, Kettunen MI, Hu DE, Witney TH, Kennedy BW, Gallagher FA, and Brindle KM (2010). Detection of tumor response to a vascular disrupting agent by hyperpolarized 13C magnetic resonance spectroscopy. *Mol Cancer Ther* **9**, 3278.
- [71] Salamanca-Cardona L and Keshari KR (2015). 13C-labeled biochemical probes for the study of cancer metabolism with dynamic nuclear polarization-enhanced magnetic resonance imaging. *Cancer Metab* **3**. <https://doi.org/10.1186/s40170-015-0136-2>.
- [72] Najac C, Chaumeil MM, Kohanbash G, Guglielmetti C, Gordon JW, Okada H, and Ronen SM (2016). Detection of inflammatory cell function using (13)C magnetic resonance spectroscopy of hyperpolarized [6-(13)C]-arginine. *Sci Rep* **6**:31397.
- [73] Chen HY, Larson PEZ, Bok RA, von Morze C, Sriram R, Delos Santos R, Delos Santos J, Gordon JW, Bahrami N, and Ferrone M, et al (2017). Assessing prostate cancer aggressiveness with hyperpolarized dual-agent 3D dynamic imaging of metabolism and perfusion. *Cancer Res* **77**, 3207.
- [74] Gallagher FA, Kettunen MI, Day SE, Hu DE, Ardenkjaer-Larsen JH, Zandt R, Jensen PR, Karlsson M, Golman K, and Lerche MH, et al (2008). Magnetic resonance imaging of pH in vivo using hyperpolarized 13C-labelled bicarbonate. *Nature* **453**, 940.
- [75] Gallagher FA, Kettunen MI, and Brindle KM (2011). Imaging pH with hyperpolarized 13C. *NMR Biomed* **24**, 1006–1015. <https://doi.org/10.1002/nbm.1742>.
- [76] Schroeder MA, Swietach P, Atherton HJ, Gallagher FA, Lee P, Radda GK, Clarke K, and Tyler DJ (2010). Measuring intracellular pH in the heart using hyperpolarized carbon dioxide and bicarbonate: a 13C and 31P magnetic resonance spectroscopy study. *Cardiovasc Res* **86**, 82.
- [77] Scholz DJ, Janich MA, Kollisch U, Schulte RF, Ardenkjaer-Larsen JH, Frank A, Haase A, Schwaiger M, and Menzel MI (2015). Quantified pH imaging with hyperpolarized (13)C-bicarbonate. *Magn Reson Med* **73**, 2274.
- [78] Drachman N, Kadlecsek S, Pourfathi M, Xin Y, Profka H, and Rizi R (2016). In vivo pH mapping of injured lungs using hyperpolarized [1-(13)C]pyruvate. *Magn Reson Med*. <https://doi.org/10.1002/mrm.26473>.
- [79] Lewis AJ, Miller JJ, McCallum C, Rider OJ, Neubauer S, Heather LC, and Tyler DJ (2016). Assessment of metformin-induced changes in cardiac and hepatic redox state using hyperpolarized[1-13C]pyruvate. *Diabetes* **65**, 3544.
- [80] Park JM, Khemtong C, Liu S-C, Hurd RE, and Spielman DM (2017). In vivo assessment of intracellular redox state in rat liver using hyperpolarized [1-(13)C]Alanine. *Magn Reson Med*. <https://doi.org/10.1002/mrm.26662>.
- [81] Karlsson M, Jensen PR, in 't Zandt R, Gisselsson A, Hansson G, Duus JO, Meier S, and Lerche MH (2010). Imaging of branched chain amino acid metabolism in tumors with hyperpolarized 13C ketoisocaproate. *Int J Cancer* **127**, 729.
- [82] Butt SA, Sogaard LV, Magnusson PO, Lauritzen MH, Laustsen C, Akeson P, and Ardenkjaer-Larsen JH (2012). Imaging cerebral 2-ketoisocaproate metabolism with hyperpolarized (13)C magnetic resonance spectroscopic imaging. *J Cereb Blood Flow Metab* **32**, 1508.
- [83] Xu HN, Kadlecsek S, Shaghghi H, Zhao H, Profka H, Pourfathi M, Rizi R, and Li LZ (2016). Differentiating inflamed and normal lungs by the apparent reaction rate constants of lactate dehydrogenase probed by hyperpolarized (13)C labeled pyruvate. *Quant Imaging Med Surg* **6**, 57.
- [84] DeVience Stephen J, Xin Lu, Proctor Julie, Rangghran Parisa, Gullapalli Rao, and Fiskum Gary M, et al (2016). Metabolic imaging of energy metabolism in traumatic brain injury using hyperpolarized [1-13C]pyruvate. ISMRM 24th Annual Meeting, Singapore; 2016.
- [85] Jannin S, Bornet A, Melzi R, and Bodenhausen G (2012). High field dynamic nuclear polarization at 6.7 T: carbon-13 polarization above 70% within 20 min. *Chem Phys Lett* **549**, 99–102. <https://doi.org/10.1016/j.cplett.2012.08.017>.
- [86] Jóhannesson H, Macholl S, and Ardenkjaer-Larsen JH (2009). Dynamic nuclear polarization of [1-13C]pyruvic acid at 4.6 tesla. *J Magn Reson* **197**, 167–175. <https://doi.org/10.1016/j.jmr.2008.12.016>.
- [87] Chen WC, Teo XQ, Lee MY, Radda GK, and Lee P (2015). Robust hyperpolarized 13C metabolic imaging with selective non-excitation of pyruvate (SNEP). *NMR Biomed* **28**, 1021–1030. <https://doi.org/10.1002/nbm.3346>.
- [88] Ardenkjaer-Larsen JH, Leach AM, Clarke N, Urbahn J, Anderson D, and Sklows TW (2011). Dynamic nuclear polarization polarizer for sterile use intent. *NMR Biomed* **24**, 927–932. <https://doi.org/10.1002/nbm.1682>.
- [89] Hu S, Lustig M, Balakrishnan A, Larson PE, Bok R, Kurhanewicz J, Nelson SJ, Goga A, Pauly JM, and Vigneron DB (2010). 3D compressed sensing for highly accelerated hyperpolarized (13)C MRSI with in vivo applications to transgenic mouse models of cancer. *Magn Reson Med* **63**, 312.
- [90] Ohliger MA, Larson PE, Bok RA, Shin P, Hu S, Tropp J, Robb F, Carvajal L, Nelson SJ, and Kurhanewicz J, et al (2013). Combined parallel and partial fourier MR reconstruction for accelerated 8-channel hyperpolarized carbon-13 in vivo magnetic resonance spectroscopic imaging (MRSI). *J Magn Reson Imaging* **38**, 701.
- [91] Walker CM, Lee J, Ramirez MS, Schellingerhout D, Millward S, and Bankson JA (2013). A catalyzing phantom for reproducible dynamic conversion of hyperpolarized [1-13C]-pyruvate. *PLoS One* **8**:e71274. <https://doi.org/10.1371/journal.pone.0071274>.
- [92] Golman K, Ardenkjaer-Larsen JH, Petersson JS, Mansson S, and Leunbach I (2003). Molecular imaging with endogenous substances. *Proc Natl Acad Sci U S A* **100**, 10435–10439. <https://doi.org/10.1073/pnas.1733836100>.
- [93] Milshteyn E, von Morze C, Reed GD, Shang H, Shin PJ, Zhu Z, Chen HY, Bok R, Goga A, and Kurhanewicz J, et al (2017). Development of high resolution 3D hyperpolarized carbon-13 MR molecular imaging techniques. *Magn Reson Imaging* **38**, 152.
- [94] Gordon JW, Vigneron DB, and Larson PEZ (2017). Development of a symmetric echo planar imaging framework for clinical translation of rapid dynamic hyperpolarized (13)C imaging. *Magn Reson Med* **77**, 826–832. <https://doi.org/10.1002/mrm.26123>.
- [95] Mayer D, Yen YF, Levin YS, Tropp J, Pfefferbaum A, Hurd RE, and Spielman DM (2010). In vivo application of sub-second spiral chemical shift imaging (CSI) to hyperpolarized 13C metabolic imaging: comparison with phase-encoded CSI. *J Magn Reson* **204**, 340.
- [96] Gordon JW, Niles DJ, Fain SB, and Johnson KM (2014). Joint spatial-spectral reconstruction and k-t spirals for accelerated 2D spatial/1D spectral imaging of 13C dynamics. *Magn Reson Med* **71**, 1435–1445. <https://doi.org/10.1002/mrm.24796>.
- [97] Cunningham CH, Lau JY, Chen AP, Geraghty BJ, Perks WJ, Roifman I, Wright GA, and Connelly KA (2016). Hyperpolarized 13C metabolic MRI of the human heart: initial experience. *Circ Res* **119**, 1177.

- [98] von Morze C, Tropp J, Chen AP, Marco-Rius I, Van Criekinge M, Skloss TW, Mammoli D, Kurhanewicz J, Vigneron DB, and Ohliger MA, et al (2018). Sensitivity enhancement for detection of hyperpolarized (13) C MRI probes with (1) H spin coupling introduced by enzymatic transformation in vivo. *Magn Reson Med* **80**, 36.
- [99] Mishkovsky M, Cheng T, Comment A, and Gruetter R (2012). Localized in vivo hyperpolarization transfer sequences. *Magn Reson Med* **68**, 349–352. <https://doi.org/10.1002/mrm.23231>.
- [100] Larson PE, Hu S, Lustig M, Kerr AB, Nelson SJ, Kurhanewicz J, Pauly JM, and Vigneron DB (2011). Fast dynamic 3D MR spectroscopic imaging with compressed sensing and multiband excitation pulses for hyperpolarized 13C studies. *Magn Reson Med* **65**, 610.
- [101] Chen HY, Larson PEZ, Gordon JW, Bok RA, Ferrone M, van Criekinge M, Carvajal L, Cao P, Pauly JM, and Kerr AB, et al (2018). Technique development of 3D dynamic CS-EPSI for hyperpolarized (13) C pyruvate MR molecular imaging of human prostate cancer. *Magn Reson Med* **80**, 2062.
- [102] Gordon JW, Hansen RB, Shin PJ, Feng Y, Vigneron DB, and Larson PEZ (2018). 3D hyperpolarized C-13 EPI with calibrationless parallel imaging. *J Magn Reson* **289**, 92–99. <https://doi.org/10.1016/j.jmr.2018.02.011>.
- [103] Feng Y, Gordon JW, Shin PJ, von Morze C, Lustig M, Larson PEZ, Ohliger MA, Carvajal L, Tropp J, and Pauly JM, et al (2016). Development and testing of hyperpolarized (13)C MR calibrationless parallel imaging. *J Magn Reson* **262**, 1.
- [104] Harris T, Elyahu G, Frydman L, and Degani H (2009). Kinetics of hyperpolarized 13C1-pyruvate transport and metabolism in living human breast cancer cells. *Proc Natl Acad Sci U S A* **106**, 18131–18136. <https://doi.org/10.1073/pnas.0909049106>.
- [105] Harrison C, Yang C, Jindal A, DeBerardinis RJ, Hooshyar MA, Merritt M, Dean Sherry A, and Malloy CR (2012). Comparison of kinetic models for analysis of pyruvate-to-lactate exchange by hyperpolarized 13 C NMR. *NMR Biomed* **25**, 1286.
- [106] Granlund Ki, Vargas H, Lyashchenko S, DeNoble P, Laudone V, Eastham J, and Keshari KR (2017). Utilizing hyperpolarized MRI in prostate cancer to assess metabolic dynamics and histopathologic grade. ISMRM 25th Annual Meeting, Honolulu, HI; 2017.
- [107] Aggarwal R, Vigneron DB, and Kurhanewicz J (2017). Hyperpolarized 1-[13C]-pyruvate magnetic resonance imaging detects an early metabolic response to androgen ablation therapy in prostate cancer. *Eur Urol* **72**, 1028–1029. <https://doi.org/10.1016/j.eururo.2017.07.022>.
- [108] Zhu Z, Gordon JW, Chen HY, Milshteyn E, Mammoli D, Carvajal L, Shin PJ, Aggarwal R, Bok R, and Kurhanewicz J, et al (2018). Human hyperpolarized 13C MRI of liver and bone metastases using both EPSI and EP acquisitions. June 16-21, 2018. Presented at the International Society Magnetic for Magnetic Resonance in Medicine 26th Annual Meeting, Paris, France; 2018.
- [109] Zhu Z, Zhu X, Ohliger M, Cao P, Tang S, Gordon JW, Carvajal L, Shin PJ, Aggarwal R, and Bok R, et al (2018). Coil combination methods for 16-channel hyperpolarized 13C spectroscopic imaging studies of liver metastases patients. June 16-12, 2018. Presented at the International Society Magnetic for Resonance in Medicine 26th Annual Meeting, Paris, France; 2018.
- [110] Park I, Larson PEZ, Gordon JW, Carvajal L, H-Y Chen R Bok, and Vigneron DB (2018). Development of methods and feasibility of using hyperpolarized carbon-13 imaging data for evaluating brain metabolism in patient studies. *Magn Reson Med* . <https://doi.org/10.1002/mrm.27077>.
- [111] Miloushev VZ, Granlund KL, Boltyanskiy R, Lyashchenko SK, DeAngelis LM, Mellinghoff IK, Brennan CW, Tabar V, Yang TJ, and Holodny AI, et al (2018). Metabolic imaging of the human brain with hyperpolarized (13)C pyruvate demonstrates (13)C lactate production in brain tumor patients. *Cancer Res* **78**, 3755.
- [112] Kelloff GJ, Hoffman JM, Johnson B, Scher HI, Siegel BA, Cheng EY, Cheson BD, O'Shaughnessy J, Guyton KZ, and Mankoff DA, et al (2005). Progress and promise of FDG-PET imaging for cancer patient management and oncologic drug development. *Clin Cancer Res* **11**, 2785.
- [113] Weber WA, Gatsonis CA, Mozley PD, Hanna LG, Shields AF, Aberle DR, Govindan R, Torigian DA, Karp JS, and Yu JQ, et al (2015). Repeatability of 18F-FDG PET/CT in advanced non-small cell lung cancer: prospective assessment in 2 multicenter trials. *J Nucl Med* **56**, 1137.
- [114] Yankeelov TE, Mankoff DA, Schwartz LH, Lieberman FS, Buatti JM, Mountz JM, Erickson BJ, Fennessy FM, Huang W, and Kalpathy-Cramer J, et al (2016). Quantitative imaging in cancer clinical trials. *Clin Cancer Res* **22**, 284.
- [115] Mankoff DA, O' Sullivan F, Barlow WE, and Krohn KA (2007). Molecular imaging research in the outcomes era: measuring outcomes for individualized cancer therapy. *Acad Radiol* **14**, 398–405. <https://doi.org/10.1016/j.acra.2007.01.005>.
- [116] Weber WA (2006). Positron emission tomography as an imaging biomarker. *J Clin Oncol* **24**, 3282–3292. <https://doi.org/10.1200/JCO.2006.06.6068>.
- [117] Olivares O, Däbritz JHM, King A, Gottlieb E, and Halsey C (2015). Research into cancer metabolomics: towards a clinical metamorphosis. *Semin Cell Dev Biol* **43**, 52–64. <https://doi.org/10.1016/j.semcdb.2015.09.008>.
- [118] Akhurst T, MacManus M, and Hicks RJ (2015). Lung cancer. *PET Clin* **10**, 147–158. <https://doi.org/10.1016/j.cpet.2014.12.002>.
- [119] Shankar LK (2012). The clinical evaluation of novel imaging methods for cancer management. *Nat Rev Clin Oncol* **9**, 738–744. <https://doi.org/10.1038/nrclinonc.2012.186>.
- [120] Henry NL and Hayes DF (2012). Cancer biomarkers. *Mol Oncol* **6**, 140–146. <https://doi.org/10.1016/j.molonc.2012.01.010>.
- [121] Cheong H, Lu C, Lindsten T, and Thompson CB (2012). Therapeutic targets in cancer cell metabolism and autophagy. *Nat Biotechnol* **30**, 671–678. <https://doi.org/10.1038/nbt.2285>.
- [122] Mankoff DA, Edmonds CE, Farwell MD, and Pryma DA (2016). Development of companion diagnostics. *Semin Nucl Med* **46**, 47–56. <https://doi.org/10.1053/j.semnuclmed.2015.09.002>.
- [123] Pien HH, Fischman AJ, Thrall JH, and Sorensen AG (2005). Using imaging biomarkers to accelerate drug development and clinical trials. *Drug Discov Today* **10**, 259–266. [https://doi.org/10.1016/S1359-6446\(04\)03334-3](https://doi.org/10.1016/S1359-6446(04)03334-3).
- [124] Smith JJ, Sorensen AG, and Thrall JH (2003). Biomarkers in imaging: realizing radiology's future. *Radiology* **227**, 633–638. <https://doi.org/10.1148/radiol.2273020518>.
- [125] Dang CV, Hamaker M, Sun P, Le A, and Gao P (2011). Therapeutic targeting of cancer cell metabolism. *J Mol Med* **89**, 205–212. <https://doi.org/10.1007/s00109-011-0730-x>.
- [126] Moghbel MC, Kostakoglu L, Zukotynski K, Chen DL, Nadel H, Niederkoher R, and Mittra E (2016). Response assessment criteria and their applications in lymphoma: part 1. *J Nucl Med* **57**, 928.
- [127] Mankoff DA, Farwell MD, Clark AS, and Pryma DA (2016). Making molecular imaging a clinical tool for precision oncology: a review. *JAMA Oncol* . <https://doi.org/10.1001/jamaoncol.2016.5084>.
- [128] Dunningham LK, Doot RK, Specht JM, Gralow JR, Ellis GK, Livingston RB, Linden WM, Gadi VK, Kurland BF, and Schubert EK, et al (2011). PET tumor metabolism in locally advanced breast cancer patients undergoing neoadjuvant chemotherapy: value of static versus kinetic measures of fluorodeoxyglucose uptake. *Clin Cancer Res* **17**, 2400.
- [129] Muzi M, O'Sullivan F, Mankoff DA, Doot RK, Pierce LA, Kurland BF, Linden HM, and Kinahan PE (2012). Quantitative assessment of dynamic PET imaging data in cancer imaging. *Magn Reson Imaging* **30**, 1203.
- [130] Huang SC (2000). Anatomy of SUV. Standardized uptake value. *Nucl Med Biol* **27**, 643–646.
- [131] McShane LM and Hayes DF (2012). Publication of tumor marker research results: the necessity for complete and transparent reporting. *J Clin Oncol* **30**, 4223–4232. <https://doi.org/10.1200/JCO.2012.42.6858>.
- [132] Shankar LK, Hoffman JM, Bacharach S, Graham MM, Karp J, Lammertsma AA, Larson S, Mankoff DA, Siegel BA, and Van den Abbeele A, et al (2006). I. National Cancer, Consensus recommendations for the use of 18F-FDG PET as an indicator of therapeutic response in patients in National Cancer Institute trials. *J Nucl Med* **47**, 1059.
- [133] Mankoff DA, Pryma DA, and Clark AS (2014). Molecular imaging biomarkers for oncology clinical trials. *J Nucl Med* **55**, 525–528. <https://doi.org/10.2967/jnumed.113.126128>.
- [134] Gerstner ER, Zhang Z, Fink JR, Muzi M, Hanna L, Greco E, Prah M, Schmainda KM, Mintz A, and Kostakoglu L, et al (2016). ACRIN 6684: Assessment of tumor hypoxia in newly diagnosed glioblastoma using 18F-FMISO PET and MRI. *Clin Cancer Res* **22**, 5079.
- [135] Kostakoglu L, Duan F, Idowu MO, Jolles PR, Bear HD, Muzi M, Cormack J, Muzi JP, Pryma DA, and Specht JM, et al (2015). A phase II study of 3'-deoxy-3'-18F-fluorothymidine PET in the assessment of early response of breast cancer to neoadjuvant chemotherapy: results from ACRIN 6688. *J Nucl Med* **56**, 1681.

- [136] Shankar LK, Van den Abbeele A, Yap J, Benjamin R, Scheutze S, and Fitzgerald TJ (2009). Considerations for the use of imaging tools for phase II treatment trials in oncology. *Clin Cancer Res* **15**, 1891–1897. <https://doi.org/10.1158/1078-0432.CCR-08-2030>.
- [137] Coleman RE, Delbeke D, Guiberteau MJ, Conti PS, Royal HD, Weinreb JC, Siegel BA, Federle MF, Townsend DW, and Berland LL, et al (2005). Concurrent PET/CT with an integrated imaging system: intersociety dialogue from the joint working group of the American College of Radiology, the Society of Nuclear Medicine, and the Society of Computed Body Tomography and Magnetic Resonance. *J Nucl Med* **46**, 1225.
- [138] Lehman CD, DeMartini W, Anderson BO, and Edge SB (2009). Indications for breast MRI in the patient with newly diagnosed breast cancer. *J Natl Compr Canc Netw* **7**, 193–201.
- [139] Zierhut ML, Yen YF, Chen AP, Bok R, Albers MJ, Zhang V, Tropp J, Park I, Vigneron DB, and Kurhanewicz J, et al (2010). Kinetic modeling of hyperpolarized  $^{13}\text{C}$ -pyruvate metabolism in normal rats and TRAMP mice. *J Magn Reson* **202**, 85.